Argonne National Laboratory

# LOAD-EQUIVALENCE PARAMETERS FOR DYNAMIC LOADING OF STRUCTURES IN THE PLASTIC RANGE

by

Carl K. Youngdahl

TABLE OF CONTENTS


| | Page |
|---|---|
| ABSTRACT | 5 |
| I. INTRODUCTION | 5 |
| II. CIRCULAR-PLATE PROBLEM | 8 |
| A. Load Range $P_y \leq P_{max} \leq P_b$ | 9 |
| B. Load Range $P_{max} > P_b$ | 10 |
| III. REINFORCED CIRCULAR CYLINDRICAL SHELL | 12 |
| A. Load Range $P_y \leq P_{max} \leq P_b$ | 13 |
| B. Load Range $P_{max} > P_b$ | 13 |
| IV. FREE-FREE BEAM | 15 |
| A. Load Range $F_y \leq F_{max} \leq F_h$ | 16 |
| B. Load Range $F_{max} > F_h$ | 17 |
| V. CIRCULAR SHELL WITH A RING LOAD | 18 |
| A. Loading Such That $\Psi\zeta < \frac{3}{2}\Psi_y\zeta_y$ | 19 |
| B. Loading Such That $\Psi\zeta = \frac{3}{2}\Psi_y\zeta_y$ at $t = t_b$ | 19 |
| VI. CONCLUSIONS | 22 |
| APPENDIXES | |
| A. Circular-plate Solution for General Pulse Shape | 23 |
| B. Solution for Reinforced Circular Cylindrical Shell for General Pulse Shape | 46 |
| C. Beam Subject to Transverse Dynamic Load of General Pulse Shape | 62 |
| REFERENCES | 71 |

## LIST OF FIGURES


| No. | Title | Page |
|---|---|---|
| 1. | Pulse Shapes | 7 |
| 2. | Problem Configurations | 8 |
| 3. | Yield Conditions | 8 |
| 4. | Effective Pressure as a Function of Maximum Pressure if $I = P_y(t_f - t_y)$ | 10 |
| 5. | Circular-plate Problem: Dependence of $W_0(t_f)/I^2$ on $P_{max}$ for Various Pulse Shapes | 12 |
| 6. | Circular-plate Problem: Dependence of $W_0(t_f)/I^2$ on $P_e$ for Various Pulse Shapes | 12 |
| 7. | Reinforced-circular-cylindrical-shell Problem: Dependence of $W_L(t_f)/I^2$ on $P_{max}$ for Various Pulse Shapes ($AH/L^2 = 0.4$) | 15 |
| 8. | Reinforced-circular-cylindrical-shell Problem: Dependence of $W_L(t_f)/I^2$ on $P_e$ for Various Pulse Shapes ($AH/L^2 = 0.4$) | 15 |
| 9. | Free-free Beam Problem: Dependence of $W_0(t_f)/I^2$ on $F_{max}$ for Various Pulse Shapes | 18 |
| 10. | Free-free Beam Problem: Dependence of $W_0(t_f)/I^2$ on $F_e$ for Various Pulse Shapes | 18 |
| 11. | Circular-cylindrical-shell Problem: Dependence of $W_0(t_f)/I^2$ on $\Psi_{max}$ for Various Pulse Shapes | 21 |
| 12. | Circular-cylindrical-shell Problem: Dependence of $W_0(t_f)/I^2$ on $\Psi_e$ for Various Pulse Shapes | 21 |
| 13. | Circular-cylindrical-shell Problem: Deviation of $(t_f - t_y)\Psi_y/I$ from Unity for Various Pulse Shapes | 22 |
| 14. | General Pressure Pulse | 23 |
| 15. | Moment and Plastic-regime Distribution in Plate | 25 |

# LOAD-EQUIVALENCE PARAMETERS FOR DYNAMIC LOADING OF STRUCTURES IN THE PLASTIC RANGE

by

Carl K. Youngdahl

## ABSTRACT

This report examines the solutions to four classical problems in dynamic plasticity--circular plate under uniform pressure, the reinforced circular cylindrical shell under uniform pressure, the free-free beam with a central concentrated force, and the circular cylindrical shell with a ring load--to determine the effect of pulse shape on final plastic deformation. It is found that there is a strong dependence on pulse shape for pulses having the same total impulse and maximum load; however, the effect of the pulse shape is virtually eliminated if the pulses have the same total impulse and effective load. The effective load is defined as the impulse divided by twice the mean time of the pulse, where the mean time is the interval between the onset of plastic deformation and the centroid of the pulse.

## I. INTRODUCTION

When experiments are performed to determine the plastic deformation of a structure produced by a dynamic loading that exceeds the yield load only for a short interval, it is important to know the effect of the pulse shape on the final deformation. This is particularly true in reactor accident simulations, where it is impossible or impractical to reproduce the actual loading conditions in an out-of-pile experiment.

Symonds,[1] in his treatment of a free-free beam acted on by a concentrated dynamic load, concluded that the final deformation for any load shape was essentially dependent only on the impulse and peak load, within an error of about 15%. However, his conclusion was based on loadings greatly in excess of the yield load, when the shape of the load is not important; the errors for loadings that produce only small plastic deformation are much larger. Hodge[2] showed that final deformation of a reinforced circular shell under uniform dynamic pressure was strongly dependent on the pulse shape. Perzyna[3] extended the solution of Hopkins and Prager[4] for a circular plate under uniform dynamic pressure with a rectangular

pulse shape to a more general class of pulse shapes and concluded that the influence of the shape on the final deflection was small. However, his conclusion was based on results for shapes that were close to the rectangular pulse in form. The analysis of Eason and Shield[5] for a long circular shell acted on by a dynamic ringload was extended by the author[6,7] to arbitrary pulse shapes. It was found that although the peak load and impulse did not provide an accurate means of eliminating the effect of the pulse shape on the final deformation, an effective load could be determined which, together with the impulse, essentially collapsed the final deformation results onto one curve.

It will be shown here that the impulse and an effective load can be used to determine the final plastic deformation for each of the above problems. For a load $\mathcal{L}(t)$, which may be a pressure, concentrated force, ring load, etc., the associated total impulse is given by

$$I = \int_{t_y}^{t_f} \mathcal{L}(t)\, dt, \tag{1}$$

where $t_y$ and $t_f$ are the times when plastic deformation begins and ends. The effective load is defined by

$$\mathcal{L}_e = \frac{I}{2t_{mean}}, \tag{2}$$

where $t_{mean}$ is the location of the centroid of the pulse and is given by

$$t_{mean} = \frac{1}{I} \int_{t_y}^{t_f} (t - t_y)\, \mathcal{L}(t)\, dt. \tag{3}$$

The time $t_y$ when plastic deformation begins is when the dynamic load first reaches the static yield load $\mathcal{L}_y$ and is consequently a known quantity. The time $t_f$ when plastic deformation ends is not known a priori, but it can be shown that

$$I \approx \mathcal{L}_y(t_f - t_y), \tag{4}$$

from which $t_f$ can be found. Relation 4 is exact for the free-free beam, reinforced-circular-shell, and circular-plate problems and is an approximation for the circular shell with a ringload. Each of the parameters I and $\mathcal{L}_e$ depends only on integrals of the loading and is insensitive to small perturbations in pulse shape. This is encouraging for experimental applications because, by contrast, peak loads and pulse durations are difficult to reproduce and measure accurately.

In what follows, the problems of the circular plate acted on by a uniform pressure, the reinforced circular shell under uniform pressure, the free-free beam with a concentrated central force, and the long circular shell with a ringload will be discussed briefly.* For each problem, the maximum plastic deformation divided by the square of the impulse is plotted as a function of the peak load and effective load for the standard pulse shapes given in Fig. 1b-f. It will be seen that there is a dependence on the pulse shape evident in the figures where the peak load is the parameter, but that this dependence is essentially eliminated if the effective load is used; i.e.,

$$W_{mf} \approx I^2 f(\mathcal{L}_e), \qquad (5)$$

where $W_{mf}$ is the maximum final deformation and f is a function that depends on the problem configuration. Closed-form solutions for the general pulse shape of Fig. 1a are available for the circular-plate and reinforced-circular-shell problems. In these cases, it is shown analytically that relation 5 is exact for small values of $(\mathcal{L}_e - \mathcal{L}_y)/\mathcal{L}_y$ and is asymptotically true for large values. The figures indicate that the error in the approximation in the intermediate range is small.

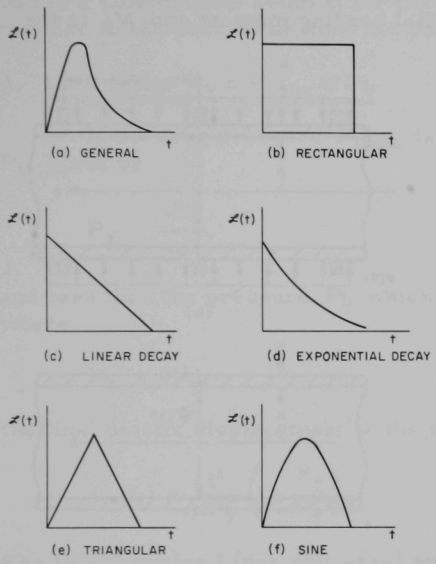


Fig. 1. Pulse Shapes. ANL Neg. No. 113-3102.

The material in each of the four problems is assumed to be rigid and perfectly plastic, and idealized yield functions are used. The use of such assumptions has proven to be very fruitful in static limit-load analysis, where the bounding theorems provide a means of bracketing the results corresponding to a more realistic material behavior. Because there are no analogous theorems for dynamic plastic deformation, the application of the idealized assumptions on material behavior is open to question. The experimental verification or rejection of the impulse and effective load as correlation parameters for final plastic deformation would also imply the verification or rejection of the usefulness of the rigid, perfectly plastic material model for dynamic analysis.

*Details of the analyses may be found in the references cited for each problem and the appendixes of this report.

## II. CIRCULAR-PLATE PROBLEM

Consider a thin circular plate of radius R and surface density $\mu$, which is loaded by a uniform pressure P(t) as in Fig. 2a. Let the plate be made of a rigid, perfectly plastic material that obeys the Tresca yield condition of Fig. 3a, where $M_r$ is the radial bending moment and $M_\phi$ is the

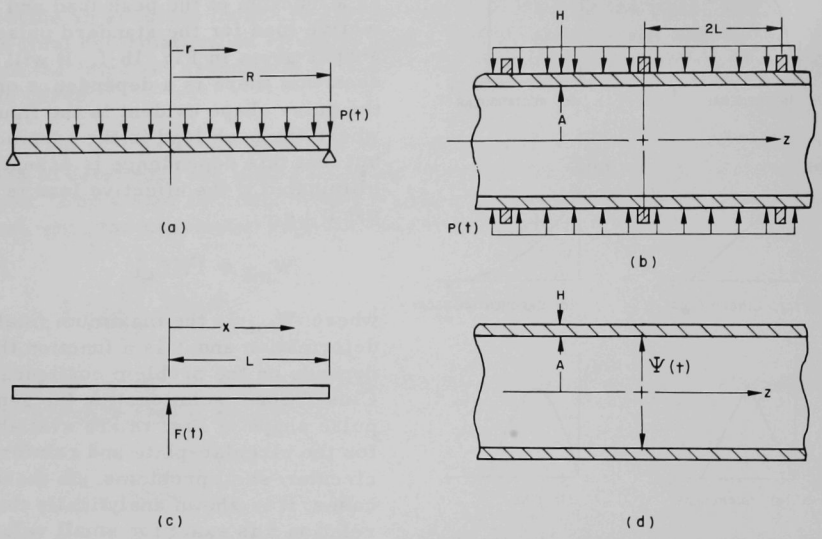


Fig. 2. Problem Configurations: (a) Circular plate loaded by a uniform pressure; (b) Reinforced circular cylindrical shell loaded by a uniform pressure; (c) Free-free beam loaded by a concentrated force; and (d) Circular cylindrical shell loaded by a ring of concentrated force. ANL Neg. No. 113-3113.

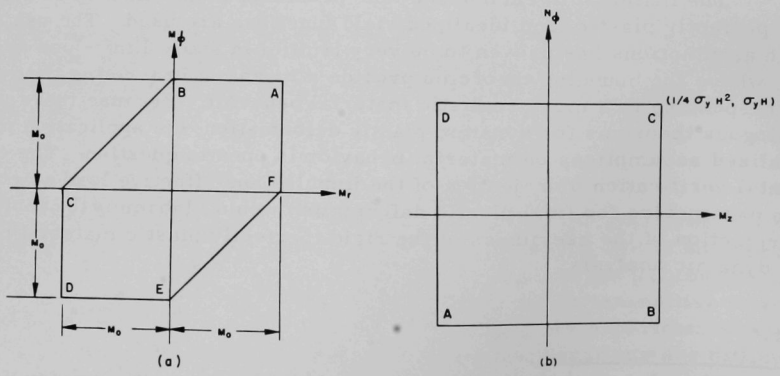


Fig. 3. Yield Conditions: (a) Tresca yield condition for circular-plate problem; and (b) Limited-interaction yield condition for circular-cylindrical-shell problems. ANL Neg. No. 113-3108 Rev. 1.

circumferential bending moment. The exact solution to this problem was presented by Hopkins and Prager[4] for a rectangular pulse shape (Fig. 1b). Perzyna[3] considered a pulse that rose instantaneously to its maximum and decayed thereafter. These results are further extended in Appendix A to obtain a closed-form solution for the general pulse shape of Fig. 1a where the rise to the peak value need not be instantaneous.

A. Load Range $P_y \leq P_{max} \leq P_b$

If the peak pressure $P_{max}$ is greater than the static yield pressure $P_y$, given by

$$P_y = \frac{6M_0}{R^2}, \tag{6}$$

and less than the pressure $P_b$ which initiates a moving hinge circle $\rho(t)$, where

$$P_b = 2P_y, \tag{7}$$

the final plastic displacement at the plate center is

$$W_0(t_f) = \frac{I^2}{\mu P_y}\left(1 - \frac{P_y}{P_e}\right). \tag{8}$$

The total impulse I (per unit area) and the effective pressure $P_e$ are defined by

$$\left.\begin{aligned} I &= \int_{t_y}^{t_f} P(t)\, dt \\ \text{and} \qquad & \\ P_e &= \frac{I}{2t_{mean}} \end{aligned}\right\}, \tag{9}$$

with

$$t_{mean} = \frac{1}{I}\int_{t_y}^{t_f} (t - t_y)\, P(t)\, dt. \tag{10}$$

Definitions 9 and 10 are the same as Eqs. 1-3 with $\mathcal{L}(t)$ specialized to P(t). Consequently, for loads in the range $P_y \leq P_{max} \leq 2P_y$, relation 5 is exact.

The time $t_f$ when the deformation ends is determined by the solution of

$$P_y(t_f - t_y) = \int_{t_y}^{t_f} P(t)\, dt. \tag{11}$$

The effective pressure is shown in Fig. 4 as a function of the maximum pressure for the standard pulse shapes of Fig. 1b-f under the restriction that the time $t_f$ at which the plastic deformation ceases can be found from Eq. 11.

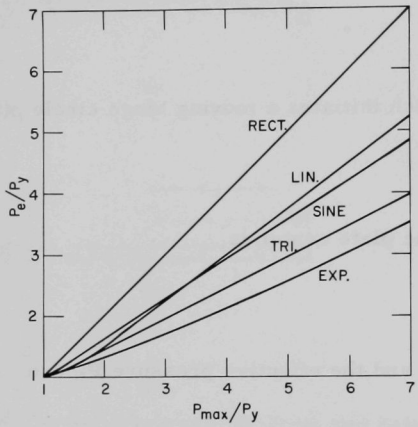


Fig. 4
Effective Pressure as a Function of Maximum Pressure if $I = P_y(t_f - t_y)$. ANL Neg. No. 113-3104.

B. Load Range $P_{max} > P_b$

At $t_b$, when P first attains the value $P_b$ given by Eq. 7, a hinge band of radius $\rho(t)$ begins to move out from the plate center and reaches a maximum $\rho_{max}$ at $t_{max}$, where $P(t_{max}) = P_{max}$. The hinge band then moves back toward the plate center, arriving there at $t_c$, which is found from

$$P_b(t_c - t_b) = \int_{t_b}^{t_c} P(t)\, dt. \tag{12}$$

For $t_b \le t \le t_{max}$, $\rho(t)$ is found from

$$P(t)[R - \rho(t)]^2[R + \rho(t)] = 2P_y R^3. \tag{13}$$

For $t_{max} \le t \le t_c$, $\rho(t)$ is the solution of

$$\int_{\beta(\rho)}^{t} P(\tau)\, d\tau = \frac{2P_y R^3[t - \beta(\rho)]}{(R+\rho)(R-\rho)^2} \tag{14}$$

with

$$\beta(\rho) = P^{-1}\left(\frac{2P_y R^3}{(R+\rho)(R-\rho)^2}\right), \qquad 0 \le \rho \le \rho_{max}, \qquad t_b \le \beta(\rho) \le t_{max}, \tag{15}$$

where $P^{-1}$ is the inverse of $P(t)$ in the interval $t_b \le t \le t_{max}$. The time $t_f$ is still given by the solution of Eq. 11. Defining

$$\left.\begin{aligned} I^* &= \int_{t_b}^{t_c} P(t)\, dt \\ \text{and} \\ P_e^* &= (I^*)^2 \Big/ \left[2\int_{t_b}^{t_c} (t - t_b)\, P(t)\, dt\right] \end{aligned}\right\}, \tag{16}$$

analogous to the definitions of I and $P_e$, we have for the final plastic deformation at the plate center

$$W_0(t_f) = \frac{I^2}{\mu}\left[\frac{1}{P_y} - \frac{1}{P_e} - \frac{1}{2}\left(\frac{I^*}{I}\right)^2\left(\frac{1}{P_b} - \frac{1}{P_e^*}\right)\right]. \tag{17}$$

Note that it is not necessary to solve the cumbersome transcendental Eqs. 13 and 14 for $\rho(t)$ in order to find $W_0(t_f)$.† Since

$$I^* \to I,\ P_e^* \to P_e \text{ as } P_e/P_y \to \infty, \tag{18}$$

Eqs. 17 and 7 yield

$$W_0(t_f) \to \frac{I^2}{\mu P_y}\left(\frac{3}{4} - \frac{P_y}{2P_e}\right) \text{ as } P_e/P_y \to \infty. \tag{19}$$

The final plastic deformation at the center of the plate divided by the square of the impulse is plotted as a function of $P_{max}$ in Fig. 5 and as a function of $P_e$ in Fig. 6 for the pulse shapes shown in Fig. 1b-f. The figures indicate that there is a significant dependence on the pulse shape if the maximum pressure is used as a parameter, but that this dependence almost disappears if $P_e$ is used. The spread in the curves for $P_{max}$ close to $P_y$ is especially large; this is perhaps the range of greatest practical interest.

†However, $W(t_f + \Delta) - W(t_f) > 0$ does depend on $\rho(t)$.

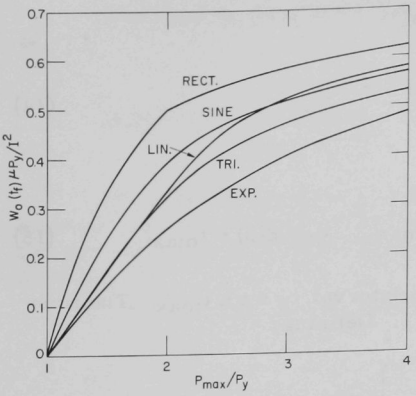


Fig. 5. Circular-plate Problem: Dependence of $W_0(t_f)/l^2$ on $P_{max}$ for Various Pulse Shapes. ANL Neg. No. 113-3111.

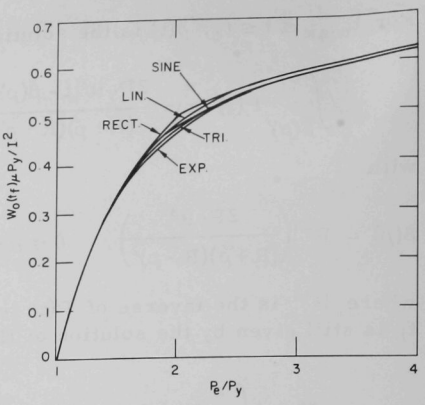


Fig. 6. Circular-plate Problem: Dependence of $W_0(t_f)/l^2$ on $P_e$ for Various Pulse Shapes. ANL Neg. No. 113-3203.

An interesting side result is that Eq. 11 has the interpretation that the average value of the load over the duration of plastic deformation is the yield load, and Eq. 12 has the interpretation that the average value of the load over the time interval in which the hinge circle moves is the initiating load for this motion.

## III. REINFORCED CIRCULAR CYLINDRICAL SHELL

Consider an infinitely long circular cylindrical shell, reinforced by equally spaced reinforcing rings and subjected to a time-dependent, uniformly distributed radial pressure (Fig. 2b). Let A, H, and $\sigma_y$ be the shell radius, thickness, and yield stress, respectively, and 2L be the distance between reinforcing rings. Only the typical half-bay $0 \leq z \leq L$ need be considered. Assume the shell material is rigid and perfectly plastic and obeys the limited interaction yield condition shown in Fig. 3b, where $N_\phi$ and $M_z$ are the circumferential stress resultant and axial bending stress resultant across the shell thickness. Hodge[2] obtained a closed-form solution to this problem for pulses that rise instantaneously to a maximum and decay thereafter. This result is broadened in Appendix B to include a closed-form solution for the general pulse shape shown in Fig. 1a.

The static yield pressure $P_y$ is given by

$$P_y = P_0\left(1 + \frac{AH}{L^2}\right), \tag{20}$$

where

$$P_0 = \frac{\sigma_y H}{A}. \tag{21}$$

The pressure $P_b$ at which a hinge band would begin to form in the vicinity of $z = L$ is given by

$$P_b = 3P_y - 2P_0. \tag{22}$$

A. Load Range $P_y \leq P_{max} \leq P_b$

For peak loads between $P_y$ and $P_b$, hinge circles are formed at $z = 0$ and $z = L$ at the time $t_y$ when the yield pressure is first attained. The maximum radial velocity $V_L$ and radial displacement $W_L$ occur at $z = L$. Corresponding to relation 4, the time $t_f$ when the deformation ends is the solution of

$$P_y(t_f - t_y) = \int_{t_y}^{t_f} P(t)\, dt \tag{23}$$

which results from

$$V_L(t_f) = 0, \qquad t_f > t_y. \tag{24}$$

The final plastic displacement at the bay midpoint is

$$W_L(t_f) = \frac{3I^2}{4\mu P_y}\left(1 - \frac{P_y}{P_e}\right), \tag{25}$$

where the impulse I (per unit area) and the effective pressure $P_e$ are defined as in Eqs. 9 and 10, and $\mu$ is the surface density of the shell material. As in the circular plate solution, for loads in the range $P_y \leq P_{max} \leq P_b$, relation 5 is exact.

B. Load Range $P_{max} > P_b$

A hinge band begins to form in the region $\zeta(t) \leq z \leq L$ at $t = t_b$ when P first attains the value $P_b$. The maximum width of the band is attained at $t = t_{max}$ when the pressure reaches its peak value. The width then decreases until $\zeta(t) = L$ at $t = t_c$, where $t_c$ is again found from Eq. 12. For $t_b \leq t \leq t_{max}$, $\zeta(t)$ is found from

$$\zeta^2(t)[P(t) - P_0] = 3L^2(P_y - P_0). \tag{26}$$

For $t_{max} \le t \le t_c$, $\zeta(t)$ is determined from the solution of

$$\zeta^2 \int_{\beta(\zeta)}^{t} [P(\tau) - P_0]\, d\tau = 3(P_y - P_0)[t - \beta(\zeta)]\, L^2 \tag{27}$$

with

$$\beta(\zeta) = P^{-1}\left[P_0 + 3(P_y - P_0)\frac{L^2}{\zeta^2}\right], \qquad \zeta_{max} \le \zeta \le L, \qquad t_{max} \ge \beta(\zeta) \ge t_b, \tag{28}$$

where $P^{-1}$ is the inverse of $P(t)$ in the interval $t_b \le t \le t_{max}$. Using $V_L(t_f) = 0$, the solution of Eq. 23 again is found to determine $t_f$. Letting I, $P_e$, $I^*$, and $P_e^*$ be defined as for the circular plate problem, we have that the final plastic deformation at the midpoint between reinforcing rings is

$$W_L(t_f) = \frac{I^2}{\mu}\left[\frac{3}{4}\left(\frac{1}{P_y} - \frac{1}{P_e}\right) - \frac{1}{4}\left(\frac{I^*}{I}\right)^2\left(\frac{1}{P_b} - \frac{1}{P_e^*}\right)\right]. \tag{29}$$

As in the circular-plate solution, it is not necessary to solve the awkward Eqs. 26 and 27 for the hinge-band motion if only the final maximum deformation is desired. The solutions given by Eqs. 17 and 29 are identical except for the numerical coefficients. Using relation 18, we have that

$$W_L(t_f) \to \frac{I^2}{\mu P_y}\left(\frac{3}{4} - \frac{P_y}{4P_b} - \frac{P_y}{2P_e}\right) \text{ as } \frac{P_e}{P_y} \to \infty, \tag{30}$$

so that in the limit, as the effective load becomes very large, we again arrive at relation 5. The ratio $P_b/P_y$ is a function of the shell geometry only, found from Eqs. 20-22 to be

$$\frac{P_b}{P_y} = 3 - \frac{2}{1 + \frac{AH}{L^2}}. \tag{31}$$

In the numerical results given here, $AH/L^2$ is taken to be 0.4 as in Ref. 2.

The final plastic deformation of the shell at the midpoint between reinforcing rings, divided by the square of the impulse, is shown as a function of $P_{max}$ in Fig. 7 and as a function of $P_e$ in Fig. 8 for the pulse shapes of Fig. 1b-f. As for the circular-plate solution, the curves are closely bunched if the effective pressure is used as the independent variable, while a strong dependence on the pulse shape is evident if the peak pressure is used.

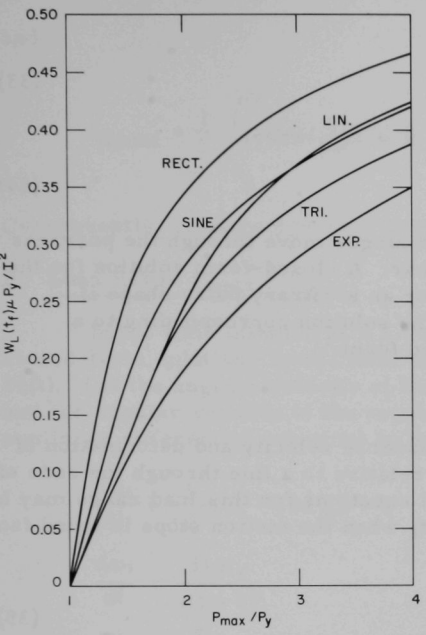


Fig. 7. Reinforced-circular-cylindrical-shell Problem: Dependence of $W_L(t_f)/I^2$ on $P_{max}$ for Various Pulse Shapes ($AH/L^2 = 0.4$). ANL Neg. No. 113-3114.

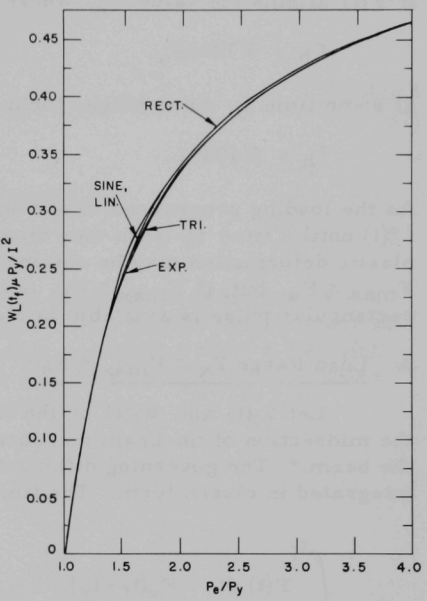


Fig. 8. Reinforced-circular-cylindrical-shell Problem: Dependence of $W_L(t_f)/I^2$ on $P_e$ for Various Pulse Shapes ($AH/L^2 = 0.4$). ANL Neg. No. 113-3204.

## IV. FREE-FREE BEAM

Consider a free-free beam of length 2L loaded at its center by a time-dependent force F(t), as shown in Fig. 2c. Assume the beam material is rigid and perfectly plastic, and let its yield moment be $M_0$. Symonds[1] presented numerical results for this problem for the rectangular, triangular, and half-sine pulse shapes of Fig. 1b, e, and f, respectively. The governing equations are derived in Appendix C. Some additional numerical results for these shapes and for the linear decay and exponential decay shapes shown in Fig. 1c and d are given here.

The yield load $F_y$ at which a plastic hinge appears at $x = 0$ is given by

$$F_y = \frac{4M_0}{L}. \tag{32}$$

If $F(t)$ attains the value $F_h$, where

$$F_h = 5.7218F_y, \tag{33}$$

at some time $t_h$ outer hinges form at $x = \pm\xi_h$, where

$$\xi_h = 0.4039L. \tag{34}$$

As the loading progresses, these outer hinges move through the positions $\pm\xi(t)$ until a time $t_c$ when they disappear. A closed-form solution for the plastic deformation may be obtained for an arbitrary pulse shape if $F_{max} \leq F_h$, but, if $F_{max} > F_h$, only the solution corresponding to a rectangular pulse is available in closed form.[1]

A. Load Range $F_y \leq F_{max} \leq F_h$

Let $V_0(t)$ and $W_0(t)$ be the transverse velocity and deformation of the midsection of the beam measured relative to a line through the ends of the beam.* The governing differential equations for this load range may be integrated in closed form. The time $t_f$ when the motion stops is found from

$$\int_{t_y}^{t_f} F(t)\,dt = F_y(t_f - t_y), \tag{35}$$

which corresponds to relation 4. The final maximum plastic deformation is

$$W_0(t_f) = \frac{3I^2}{2\gamma LF_y}\left(1 - \frac{F_y}{F_e}\right), \tag{36}$$

where the total impulse $I$ and effective force $F_e$ are defined analogous to Eqs. 1, 2, and 3 by

$$I = \int_{t_y}^{t_f} F(t)\,dt,$$

$$F_e = \frac{I}{2t_{mean}}, \tag{37}$$

(Contd.)

*Because the beam is unsupported, it also has a rigid body motion. Symonds[1] takes the angular deformation $\theta$ at the center of the beam as a measure of the plastic deformation. For $F_{max} \leq F_h$, $\theta$ and $W_0(t)$ differ only by a constant factor L; but for $F_{max} > F_h$, the relationship depends on $\xi(t)$.

and

$$t_{mean} = \frac{1}{I} \int_{t_y}^{t_f} (t - t_y)\, F(t)\, dt. \qquad \text{(Contd.)} \quad (37)$$

Consequently, relation 5 is exact for $F_{max} \leq F_h$.

B. Load Range $F_{max} > F_h$

In the time interval $t_y \leq t \leq t_h$, the differential equations have a closed-form solution. In the interval $t_h \leq t \leq t_c$, plastic hinges occur at $\pm\xi(t)$. Let the angular velocity of the beam segment* $0 \leq x < \xi$ be $\omega_0(t)$, and the angular velocity of the segment $\xi < x \leq L$ be $\omega_1(t)$. The coupled nonlinear differential equations to be solved are

$$\left.\begin{aligned} \frac{d\omega_0}{dt} &= \frac{3}{\gamma\xi^3}[\xi F - 2LF_y], \\ \frac{d\omega_1}{dt} &= \frac{3LF_y}{\gamma(L-\xi)^3}, \\ \frac{dV_0}{dt} &= \frac{1}{2}\left[\frac{F}{\gamma\xi} + \xi\frac{d\omega_0}{dt} + (L-\xi)\frac{d\omega_1}{dt}\right], \\ \frac{dW_0}{dt} &= V_0, \end{aligned}\right\} \quad (38)$$

and

$$\frac{d\xi}{dt} = \frac{1}{\gamma\xi^2(\omega_0 - \omega_1)}\left[3F_yL - \frac{3\xi^2F_yL}{2(L-\xi)^2} - \xi F\right].$$

The time $t_c$ is determined from the condition that $\omega_0(t_c) = \omega_1(t_c)$. This system of equations is easily solved on a computer. In the time interval $t_c \leq t \leq t_f$, the governing differential equations have closed-form solutions. It is shown in Ref. 1, using conservation of momentum, that Eq. 35 holds regardless of the pulse shape. In other words, even though a closed-form solution to differential Eqs. 38 cannot be found, relation 4 is again exact.

The ratio $W_0(t_f)/I^2$, given by Eq. 36 for $F_{max} \leq F_h$ and by the computer solution of the differential equations for $F_{max} \geq F_h$, is shown as a function of $F_{max}$ and $F_e$ in Figs. 9 and 10, respectively. The resemblance to the results of the previous two problems is evident.

*Because of symmetry, only the right half of the beam need be considered.

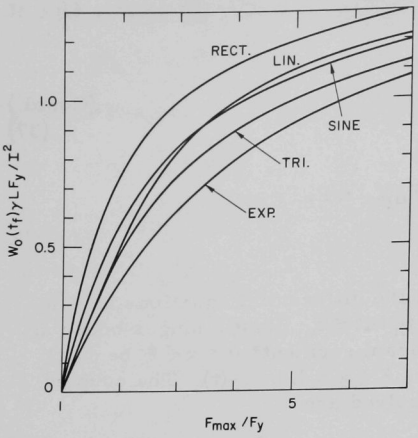


Fig. 9. Free-free Beam Problem: Dependence of $W_0(t_f)/I^2$ on $F_{max}$ for Various Pulse Shapes. ANL Neg. No. 113-3110.

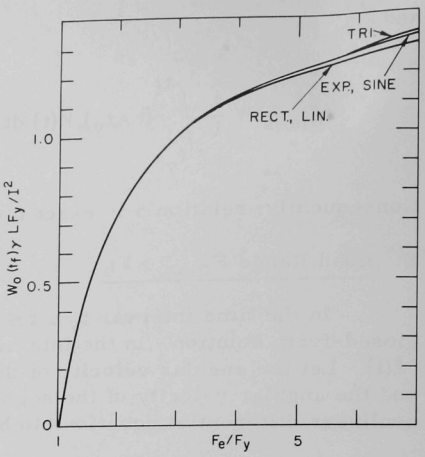


Fig. 10. Free-free Beam Problem: Dependence of $W_0(t_f)/I^2$ on $F_e$ for Various Pulse Shapes. ANL Neg. No. 113-3202.

## V. CIRCULAR SHELL WITH A RING LOAD

Consider an infinitely long circular shell which is axially unrestrained and loaded by a dynamic concentrated ring load $\Psi(t)$ at the cross-section z = 0 (Fig. 2d). Assume the material of the shell is rigid and perfectly plastic and obeys the limited-interaction yield condition shown in Fig. 3b. Eason and Shield[5] obtained a closed-form solution for the plastic deformation corresponding to the rectangular pulse of Fig. 1b and gave numerical results for the triangular pulse of Fig. 1e. The author[6,7] obtained a numerical solution for arbitrary pulse shapes, including those of Fig. 1c, d, and f.

The static limit load $\Psi_y$ is given by

$$\Psi_y = \frac{2\sigma_y H^{3/2}}{A^{1/2}}, \tag{39}$$

where $\sigma_y$, H, and A are the yield stress, thickness, and radius of the shell, respectively. Because of symmetry, only the half $z \geq 0$ of the shell need be considered. At $t = t_y$, when the yield load is first attained, plastic-hinge circles appear at z = 0 and $z = \zeta_y$, where

$$\zeta_y = \sqrt{AH}. \tag{40}$$

As the loading progresses, the outer hinge circle moves through the positions $\zeta(t)$. If, at some time $t_b$,

$$\Psi(t_b)\zeta(t_b) = \tfrac{3}{2}\Psi_y\zeta_y, \tag{41}$$

the outer hinge circle begins to broaden into a hinge band occupying the region $\zeta_1(t) \le z \le \zeta_2(t)$. As the load passes through a maximum and then decreases, the width of the hinge band attains its maximum and eventually shrinks to a hinge circle again at time $t_c$. Unlike the first two problems treated here, the occurrence of a hinge band depends not only on the magnitude of the pulse but also on its shape. For instance, it may be shown that a hinge band cannot occur for a rectangular pulse[5] or any other pulse shape that attains its maximum value instantaneously.[6]

A. Loading Such That $\Psi\zeta < \frac{3}{2}\Psi_y\zeta_y$

If Eq. 41 is never satisfied during the deformation, the outer hinge location $\zeta(t)$ and the radial velocity and displacement at $z = 0$, $V_0(t)$ and $W_0(t)$, respectively, are the solutions of the coupled nonlinear differential equations

$$\left.\begin{aligned} \frac{d\zeta}{dt} &= \frac{1}{\mu V_0}\left[-2\Psi + \Psi_y\left(\frac{3\zeta_y}{\zeta} - \frac{\zeta}{\zeta_y}\right)\right], \\ \mu\frac{dV_0}{dt} &= \frac{4\Psi}{\zeta} - \Psi_y\left(\frac{3\zeta_y}{\zeta^2} - \frac{1}{\zeta_y}\right), \end{aligned}\right\} \tag{42}$$

and

$$\left.\frac{dW_0}{dt} = V_0,\right\}$$

where $\mu$ is the surface density of the shell. The only pulse shape for which a solution of Eqs. 42 is available is the rectangular pulse.

B. Loading Such That $\Psi\zeta = \frac{3}{2}\Psi_y\zeta_y$ at $t = t_b$

During the intervals $t_y \le t \le t_b$ and $t_c \le t \le t_f$ when there is no hinge band, differential Eqs. 42 are applicable. For $t_b \le t \le t_{max}$, the inner edge of the hinge band is given by

$$\zeta_1(t) = \frac{3\Psi_y\zeta_y}{2\Psi(t)}, \tag{43}$$

while $V_0(t)$, $W_0(t)$, and $V_1(t)$ (which is defined as $V(z,t)$ at $z = \zeta_1$) are found from the solutions of the differential equations

$$\frac{d}{dt}\left(\frac{V_0 - V_1}{\zeta_1}\right) = \frac{6}{\zeta_1^3}\left(\Psi\zeta_1 - \Psi_y\zeta_y\right), \tag{44}$$

$$\mu\frac{dV_0}{dt} = \frac{4\Psi}{\zeta_1} - \Psi_y\left(\frac{\Psi_y\zeta_y}{\zeta_1^2} + \frac{1}{\zeta_y}\right), \tag{45}$$

and

$$\frac{dW_0}{dt} = V_0.$$

An auxiliary function $Q(z)$ is given by

$$Q(\zeta_1) = \frac{\mu V_1\zeta_y}{\Psi_y} + t, \tag{46}$$

treating $t$ as a function of $\zeta_1$ rather than the reverse. The outer edge of the hinge band is then given by

$$Q(\zeta_2(t)) = t. \tag{47}$$

For $t_{max} \leq t \leq t_c$, Eq. 43 no longer applies, but Eq. 46 used with Eqs. 45 yields four relations for $\zeta_1$, $V_0$, $V_1$, and $W_0$, while $\zeta_2$ is still found from Eq. 47. A closed-form solution for an arbitrary pulse shape is available for the interval $t_b \leq t \leq t_c$ when the hinge band exists.[6] However, since the solution is awkward to evaluate and there is no corresponding solution for the initial and final stages of the deformation, it is easier to solve the entire problem using a standard computer subroutine for simultaneous differential equations.

The numerical results for the quantity $W_0(t_f)/I^2$ are plotted as a function of $\Psi_{max}$ and $\Psi_e$ in Figs. 11 and 12, respectively, for the standard pulse shapes. The total impulse I (per unit circumference) and the effective circumferential load $\Psi_e$ are defined analogously to Eqs. 1, 2, and 3 by

$$I = \int_{t_y}^{t_f} \Psi(t)\, dt, \qquad \Psi_e = \frac{I}{2t_{mean}}, \tag{48}$$

and

$$t_{mean} = \frac{1}{I}\int_{t_y}^{t_f} (t - t_y)\,\Psi(t)\, dt. \tag{49}$$

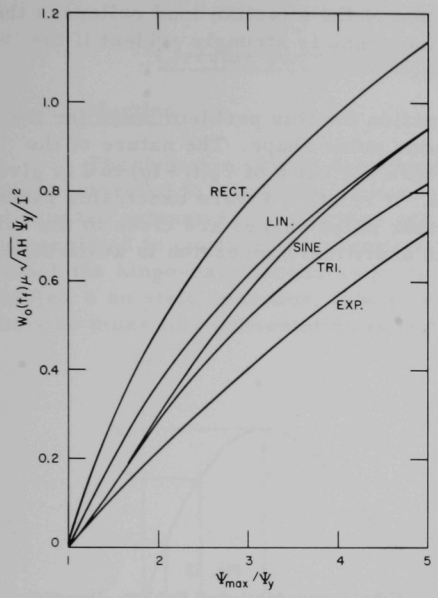


Fig. 11

Circular-cylindrical-shell Problem: Dependence of $W_0(t_f)/I^2$ on $\Psi_{max}$ for Various Pulse Shapes. ANL Neg. No. 113-3105 Rev. 1.

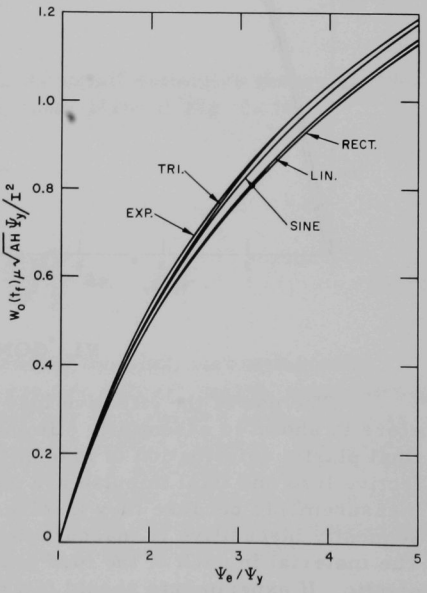


Fig. 12

Circular-cylindrical-shell Problem: Dependence of $W_0(t_f)/I^2$ on $\Psi_e$ for Various Pulse Shapes. ANL Neg. No. 113-3112 Rev. 1.

As for the other three problems, the use of the effective load collapses the curves, while a dependence on the pulse shape is strongly evident if the maximum load is used as a parameter.

Relation 4 is only an approximation for this problem, even for the closed-form solution for the rectangular pulse shape. The nature of the approximation is shown in Fig. 13, where the ratio of $\Psi_y(t_f - t_y)$ to I is given for the various standard pulse shapes. If relation 4 were exact, this ratio would be unity. The curves for the other pulse shapes are close to the curve for the rectangular pulse for which an analytical expression is available.[6]

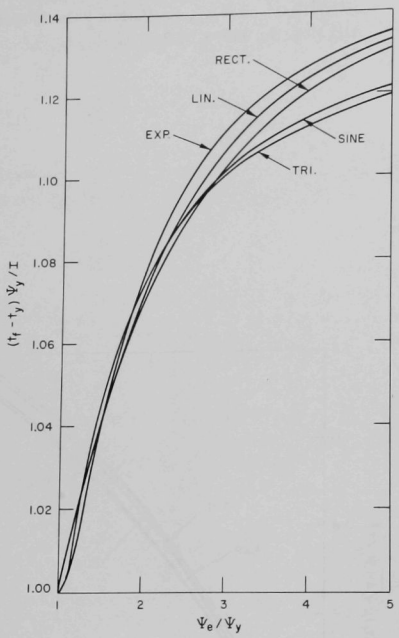


Fig. 13
Circular-cylindrical-shell Problem: Deviation of $(t_f - t_y)\Psi_y/I$ from Unity for Various Pulse Shapes. ANL Neg. No. 113-3106.

## VI. CONCLUSIONS

The use of the effective load and total impulse as correlation parameters is shown to essentially eliminate the dependence on pulse shape of the final plastic deformation of four different structural configurations. The effective load and total impulse are easily determined from pressure-time measurements because they involve only integrals of the loading and are consequently insensitive to inaccuracies in pressure-transducer measurements. The material in each of the four problems is assumed to be rigid, perfectly plastic. If experiments should fail to confirm correlation 5, it would indicate that the rigid-plastic idealization may not be useful in dynamic plasticity.

# APPENDIX A

## Circular-plate Solution for General Pulse Shape

### 1. Introduction

The dynamic plastic deformation of a simply supported circular plate subjected to a uniform pressure* with a rectangular pulse shape is discussed extensively by Hopkins and Prager.[4] Their analysis will be generalized to cover the arbitrary pressure pulse shape of Fig. 14 for which the hinge-band motion is more complicated. Some of the discussion in Ref. 4 on yield condition, flow rule, and plastic regimes will be repeated here to make this presentation reasonably complete.

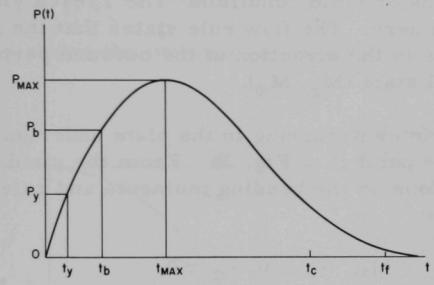


Fig. 14
General Pressure Pulse.
ANL Neg. No. 113-3222.

### 2. Statement of Problem

Under the usual assumptions of the small deflection theory of thin plates, the equation of motion of the circular plate of Fig. 2a is

$$\frac{\partial}{\partial r}(rM_r) - M_\phi = rQ$$

$$= \int_0^r \left[-P + \mu \frac{\partial^2 W}{\partial t^2}\right] r \, dr, \qquad (A.1)$$

where $M_r$, $M_\phi$, and Q are the radial bending moment, circumferential bending moment, and vertical shear force per unit arc length, respectively, P is the applied pressure, $\mu$ is the mass per unit surface area, and W is the downward deflection of points lying in the middle surface. The quantities $M_r$, $M_\phi$, Q, and W are functions of radius r and time t, while P will be taken to be a function of time only. Let the plate radius be R, the lateral velocity of the plate be denoted by V(r,t), and the radial and circumferential rates of curvature be denoted by $\kappa_r$ and $\kappa_\phi$, respectively. Then

*Conroy[9] considers a uniform pressure distributed over a central circular region.

$$V = \frac{\partial W}{\partial t}, \tag{A.2a}$$

$$\kappa_r = -\frac{\partial^2 V}{\partial r^2}, \tag{A.2b}$$

and

$$\kappa_\phi = -\frac{1}{r}\frac{\partial V}{\partial r}. \tag{A.2c}$$

The locus of points in $M_r$, $M_\phi$ space representing all possible yield states is called the yield locus or yield condition. The Tresca yield condition of Fig. 3a will be used here. The flow rule states that the flow vector with components $\kappa_r$, $\kappa_\phi$ is in the direction of the outward perpendicular to the yield locus at the yield state ($M_r$, $M_\phi$).

The three plastic regimes occurring in the plate under uniform load are point A, segment AB, and point B of Fig. 3a. From the yield condition and the flow rule, the conditions on the bending moments and rates of curvature for these regimes are:

Regime A: $M_r = M_\phi = M_0$, $\kappa_r \geq 0$, $\kappa_\phi \geq 0$; (A.3a)

Regime AB: $0 < M_r < M_0$, $M_\phi = M_0$, $\kappa_r = 0$, $\kappa_\phi \geq 0$; (A.3b)

Regime B: $M_r = 0$, $M_\phi = M_0$, $\kappa_\phi \geq -\kappa_r \geq 0$. (A.3c)

During the plastic deformation of the plate subjected to uniform pressure

$$M_\phi = M_0, \qquad 0 \leq r \leq R. \tag{A.4}$$

The simply supported outer edge of the plate is in Regime B; i.e.,

$$V = W = M_r = 0 \text{ at } r = R. \tag{A.5}$$

For load histories such that no hinge band appears, the center of the plate is in Regime A, so that

$$M_r = M_0 \text{ at } r = 0, \tag{A.6}$$

while the remainder of the plate is in Regime AB, which means, using Eqs. A.2 and A.3b,

$$0 < M_r < M_0, \quad \frac{\partial^2 V}{\partial r^2} = 0, \quad \frac{\partial V}{\partial r} \leq 0 \qquad \text{for } 0 < r < R. \tag{A.7}$$

If a hinge band of radius $\rho(t)$ grows out from the center of the plate, the entire band is in Regime A so that

$$M_r = M_0, \quad \frac{\partial^2 V}{\partial r^2} \leq 0, \quad \frac{\partial V}{\partial r} \leq 0 \qquad \text{for } 0 \leq r \leq \rho, \tag{A.8}$$

while the remainder of the plate is still in Regime AB;

$$0 < M_r < M_0, \quad \frac{\partial^2 V}{\partial r^2} = 0, \quad \frac{\partial V}{\partial r} \leq 0 \qquad \text{for } \rho < r < R. \tag{A.9}$$

Figure 15 shows the moment and plastic-regime distribution in the plate.

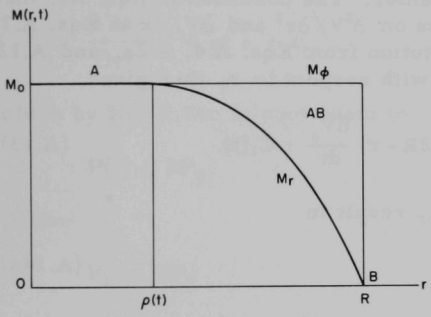


Fig. 15. Moment and Plastic-regime Distribution in Plate. ANL Neg. No. 113-3223.

The initial condition of the motion is that the plate is at rest until time $t_y$ when the yield load is first reached. Consequently,

$$V(r,t_y) = W(r,t_y) = 0. \tag{A.10}$$

Equation of motion A.1 must be solved subject to initial conditions A.10 and boundary conditions and restrictions A.4-A.7 if there is no hinge band. If a hinge band appears, Eqs. A.6 and A.7 are replaced by Eqs. A.8 and A.9.

The restrictions on the continuity of $M_r$, $M_\phi$, W, and their derivatives are discussed in detail in Ref. 4. The arguments will not be repeated here; the conclusions pertinent to this problem are: W, V, $M_r$, and $\partial W/\partial r$ are continuous in r and t, but across a moving hinge circle $\rho(t)$, the discontinuity conditions

$$\left\{\frac{\partial V}{\partial r}\right\} + \frac{d\rho}{dt}\left\{\frac{\partial^2 W}{\partial r^2}\right\} = 0, \tag{A.11a}$$

$$\left\{\frac{\partial V}{\partial t}\right\} + \frac{d\rho}{dt}\left\{\frac{\partial V}{\partial r}\right\} = 0, \tag{A.11b}$$

and

$$\left\{\frac{\partial M_r}{\partial t}\right\} + \frac{d\rho}{dt}\left\{\frac{\partial M_r}{\partial r}\right\} = 0, \tag{A.11c}$$

must be satisfied. In Eqs. A.11, $\{f\}$ denotes the discontinuity in f across $\rho$.

3. Solution for No Hinge Band ($P_{max} \leq P_b$)

Guided by the static limit analysis,[8] take the initial velocity distribution as

$$V(r,t) = V_0(t)\frac{R - r}{R}, \tag{A.12}$$

where $V_0$ is the velocity at the plate center. The condition in Eqs. A.5 that V vanishes at r = R and the conditions on $\partial^2 V/\partial r^2$ and $\partial V/\partial r$ in Eqs. A.7 are satisfied by Eq. A.12. The substitution from Eqs. A.4, A.2a, and A.12 into Eqs. A.1, followed by integration with respect to r, then gives

$$r(M_r - M_0) = -\frac{1}{6}r^3 P + \frac{\mu r^3}{12R}(2R - r)\frac{dV_0}{dt} + C_1(t). \tag{A.13}$$

Boundary conditions A.5 and A.6 on $M_r$ result in

$$C_1(t) = 0, \tag{A.14a}$$

$$\frac{dV_0}{dt} = \frac{2}{\mu}[P(t) - P_y], \tag{A.14b}$$

and

$$M_r = \frac{R - r}{6R}[P(t)r^2 + P_y(R^2 + Rr - r^2)], \tag{A.14c}$$

where the static yield load $P_y$ is[8]

$$P_y = \frac{6M_0}{R^2}. \tag{A.15}$$

The solution of differential equations A.2a and A.14b is, using Eq. A.12 and initial condition A.10,

$$V_0(t) = \frac{2}{\mu}\int_{t_y}^{t}[P(\tau) - P_y]\,d\tau, \tag{A.16a}$$

$$W_0(t) = \frac{2}{\mu} \int_{t_y}^{t} (t - \tau)[P(\tau) - P_y]\, d\tau, \tag{A.16b}$$

and

$$W(r,t) = W_0(t) \frac{R - r}{R}, \tag{A.16c}$$

where $W_0(t)$ is the displacement at the plate center.

Because $M_r = M_0$ and $\partial M_r/\partial r = 0$ at $r = 0$ (see Eq. A.1), the condition that $M_r \leq M_0$ throughout the region $0 < r < R$ will be satisfied if $r = 0$ is a local maximum of $M_r$; i.e.,

$$\frac{\partial^2 M_r}{\partial r^2} < 0 \text{ at } r = 0, \tag{A.17}$$

which by Eq. A.14c is equivalent to

$$P(t) < 2P_y. \tag{A.18}$$

Define

$$P_b = 2P_y \tag{A.19}$$

as the load at which a hinge band is initiated. The condition that P(t) does not produce a hinge band is then

$$P_{max} < P_b. \tag{A.20}$$

The plastic deformation ends at time $t_f$ when $V(r,t)$ vanishes. By Eqs. A.12 and A.16a, $t_f$ is found from the solution of

$$\int_{t_y}^{t_f} P(t)\, dt = P_y(t_f - t_y). \tag{A.21}$$

Equation A.21 has the interpretation that the average pressure over the interval of deformation is the yield load.

Define the impulse I per unit area, the mean time $t_{mean}$ of the pulse, and the effective pressure $P_e$ by

$$I = \int_{t_y}^{t_f} P(t)\, dt, \tag{A.22a}$$

$$t_{mean} = \frac{1}{I} \int_{t_y}^{t_f} (t - t_y)\, P(t)\, dt, \tag{A.22b}$$

and

$$P_e = \frac{I}{2t_{mean}}. \tag{A.22c}$$

From Eqs. A.16b, A.21, and A.22, the final plastic deformation at $r = 0$ is found to be

$$W_0(t_f) = \frac{I^2}{\mu P_y} \left(1 - \frac{P_y}{P_e}\right), \tag{A.23}$$

and $W(r,t_f)$ is easily determined from Eqs. A.16c and A.23.

4. Solution for Deformation with Hinge Band ($P_{max} > P_b$)

a. Interval $t_y \leq t \leq t_b$

The solution given by Eqs. A.14c and A.16 is applicable up to the time $t_b$ when the pressure first reaches the value $P_b$ and $\partial^2 M_r/\partial r^2 = 0$ at $r = 0$. At $t_b$, a hinge circle $\rho(t)$ separating the region of the plate in Regime A from the region in Regime AB begins to move out from the origin.

b. Interval $t_b \leq t \leq t_{max}$

The substitution from Eqs. A.4 and A.8 for $M_\phi$ and $M_r$ into partial differential equation A.1 results in the integral vanishing for arbitrary r in the region $0 \leq r \leq \rho(t)$. This implies that the integrand must be identically zero, or,

$$\mu \frac{\partial V}{\partial t} = P(t). \tag{A.24}$$

The solution of Eq. A.24 is

$$\mu V(r,t) = \int_{t_b}^{t} P(\tau)\, d\tau + \Omega(r); \qquad 0 \leq r \leq \rho(t), \tag{A.25}$$

where $\Omega(r)$ is an arbitrary function determined from the continuity of the velocity at the edge of the region. Letting $V_\rho(t)$ be the instantaneous lateral velocity at the hinge circle, i.e.,

$$V_\rho(t) = V(\rho(t),t), \tag{A.26}$$

$\Omega$ is found from

$$\Omega(\rho) = \mu V_\rho - \int_{t_b}^{t} P(\tau)\, d\tau, \tag{A.27}$$

where t is viewed as a function of $\rho$ rather than the converse.

Since the integrand in Eq. A.1 is identically zero for $0 < r < \rho(t)$, the governing partial differential equation for the region $\rho(t) < r < R$ is, using Eqs. A.4, A.15, and A.2a,

$$\frac{\partial}{\partial r}(rM_r) = \frac{1}{6} P_y R^2 + \int_{\rho}^{r} \left[-P(t) + \mu \frac{\partial V}{\partial t}\right] r\, dr. \tag{A.28}$$

Using relations A.9 and A.5, the expression for V(r,t), analogous to Eq. A.12 which applies up to $t_b$, will be taken as

$$V(r,t) = V_\rho(t) \frac{R - r}{R - \rho(t)}, \quad \rho \le r \le R, \quad t_b \le t \le t_c, \tag{A.29}$$

where $t_c$ is the time when the hinge band shrinks to the origin. Integration of Eq. A.28 with respect to r then gives

$$rM_r = \frac{r}{6}\left[R^2 P_y + (3\rho^2 - r^2) P + (Rr^2 - 3R\rho^2 - \frac{1}{2} r^3 + 2\rho^3)\mu \frac{d}{dt}\left(\frac{V_\rho}{R - \rho}\right)\right] + C_2(t). \tag{A.30}$$

The boundary condition on $M_r$ given in Eq. A.5 and the continuity of $M_r$ at $r = \rho$ are used to obtain

$$C_2(t) = \frac{\rho^3 R}{6(R - \rho)(R + 3\rho)}\left[\frac{(3\rho - 4R) R^2 P_y}{(R - \rho)^2} + (2R + \rho) P\right], \tag{A.31a}$$

$$\frac{d}{dt}\left(\frac{V_\rho}{R - \rho}\right) = \frac{2}{\mu(R - \rho)(R + 3\rho)}\left[-\frac{R^3 P_y}{(R - \rho)^2} + (R + 2\rho) P\right], \tag{A.31b}$$

and

$$M_r = \frac{R - r}{6r(R-\rho)(R+3\rho)} \left[ (R^3 r + R^2 r^2 - R r^3 - 4R\rho^3 + 3\rho^4) \frac{R^2 P_y}{(R-\rho)^2} \right.$$

$$\left. + (Rr + 2R\rho + 2r\rho + \rho^2)(r-\rho)^2 P \right],$$

$$\rho \leq r \leq R, \quad t_b \leq t \leq t_c. \tag{A.31c}$$

The condition that $M_r$ should not exceed $M_0$ in the region $\rho \leq r \leq R$ implies

$$\frac{\partial^2 M_r}{\partial r^2} \leq 0 \text{ at } r = \rho^+. \tag{A.32}$$

Using Eq. A.31c, this is equivalent to

$$(R+\rho)(R-\rho)^2 P \leq 2P_y R^3, \quad t_b \leq t \leq t_c. \tag{A.33}$$

When the hinge band is initiated, the radius of the hinge circle is zero and the pressure has the value $2P_y$ by Eq. A.19. Consequently, the equality in expression A.33 holds at $t = t_b$. We will hypothesize that the equality continues to hold in the entire interval $t_b \leq t \leq t_{max}$, so that $\rho(t)$ is determined by the solution of the cubic equation

$$[R + \rho(t)][R - \rho(t)]^2 = \frac{2P_y R^3}{P(t)}, \quad t_b \leq t \leq t_{max}. \tag{A.34}$$

The basis of this hypothesis is as follows: The differentiation of Eq. A.34 yields

$$\frac{d\rho}{dt} = \frac{2P_y R^3}{(R-\rho)(R+3\rho)\,P^2} \frac{dP}{dt}. \tag{A.35}$$

Since $d\rho/dt$ and $dP/dt$ have the same sign and vanish at the same time, $\rho(t)$ attains its maximum when $P = P_{max}$. Equations A.34 and A.35 imply that the hinge circle is "pushed" out from the origin to its extreme position as the pressure increases from $P_b$ to $P_{max}$. A value of $\rho$ less than that which satisfies Eq. A.34 would cause relation A.33 to be violated. It can be shown that a solution for the plate deformation obtained by using Eq. A.34 satisfies the differential equations, the boundary conditions, and discontinuity conditions A.11, and is therefore the correct solution.

Combining Eq. A.34 with Eq. A.31c gives, using Eq. A.15,

$$\frac{M_r}{M_0} = 1 - \frac{R(r+\rho)(r-\rho)^3}{r(R+\rho)(R-\rho)^3}, \qquad \rho \le r \le R, \qquad t_b \le t \le t_{max}, \tag{A.36}$$

while Eq. A.31b reduces to

$$\frac{d}{dt}\left(\frac{V_\rho}{R-\rho}\right) = \frac{P}{\mu(R-\rho)}. \tag{A.37}$$

We integrate Eq. A.37 to obtain

$$V_\rho(t) = [R - \rho(t)]\left[\frac{1}{\mu}\int_{t_b}^{t} \frac{P(\tau)}{R-\rho(\tau)}\, d\tau + \frac{V_\rho(t_b)}{R-\rho(t_b)}\right]. \tag{A.38}$$

Since $V_\rho(t_b) = V_0(t_b)$ and $\rho(t_b) = 0$, we have from Eq. A.16a that

$$V_\rho(t_b) = \frac{2}{\mu}\int_{t_y}^{t_b} [P(\tau) - P_y]\, d\tau. \tag{A.39}$$

Substituting from Eqs. A.38 and A.39 into Eq. A.29 gives

$$V(r,t) = \frac{R-r}{\mu R}\left[R\int_{t_b}^{t} \frac{P(\tau)}{R-\rho(\tau)}\, d\tau + 2\int_{t_y}^{t_b} [P(\tau) - P_y]\, d\tau\right],$$

$$\rho \le r \le R, \qquad t_b \le t \le t_{max}. \tag{A.40}$$

The plate displacement is then found by integrating the velocity and applying the continuity conditions at $t_b$, using Eqs. A.16b,c. The result is

$$W(r,t) = \frac{R-r}{\mu R}\left\{R\int_{t_b}^{t} \frac{(t-\tau)\,P(\tau)}{R-\rho(\tau)}\, d\tau + 2\int_{t_y}^{t_b} (t-\tau)[P(\tau) - P_y]\, d\tau\right\},$$

$$\rho \le r \le R, \qquad t_b \le t \le t_{max}. \tag{A.41}$$

We return now to the region $0 \le r \le \rho$ in order to determine $\Omega(r)$ from the continuity of the velocity at the hinge circle. The solution $\rho(t)$ to Eq. A.34 can be inverted to give

$$t = \beta(\rho), \qquad 0 \le \rho \le \rho_{max}, \qquad t_b \le t \le t_{max}, \tag{A.42}$$

with

$$\beta(\rho) = P^{-1}\left(\frac{2P_y R^3}{(R+\rho)(R-\rho)^2}\right), \qquad P_b \le P(t) \le P_{max}. \tag{A.43}$$

By Eqs. A.27, A.38, A.39, and A.42, we have

$$\Omega(\rho) = (R-\rho)\left[\int_{t_b}^{\beta(\rho)} \frac{P(\tau)}{R-\rho(\tau)}\, d\tau + 2\int_{t_y}^{t_b} [P(\tau) - P_y]\, d\tau\right]$$

$$- \int_{t_b}^{\beta(\rho)} P(\tau)\, d\tau, \qquad 0 \le \rho \le \rho_{max}. \tag{A.44}$$

Substituting this result into Eq. A.25 then gives

$$\mu V(r,t) = \int_{\beta(r)}^{t} P(\tau)\, d\tau + (R-r)\int_{t_b}^{\beta(r)} \frac{P(\tau)}{R-\rho(\tau)}\, d\tau$$

$$+ \frac{2(R-r)}{R}\int_{t_y}^{t_b} [P(\tau) - P_y]\, d\tau,$$

$$0 \le r \le \rho, \qquad t_b \le t \le t_c. \tag{A.45}$$

The displacement is found by integrating $V(r,t)$ with respect to time and applying continuity conditions at $t = t_b$; the result is

$$\mu W(r,t) = \int_{\beta(r)}^{t} (t-\tau)\, P(\tau)\, d\tau + (R-r)\int_{t_b}^{\beta(r)} \frac{(t-\tau)\, P(\tau)}{R-\rho(\tau)}\, d\tau$$

$$+ \frac{2(R-r)}{R}\int_{t_y}^{t_b} (t-\tau)[P(\tau) - P_y]\, d\tau,$$

$$0 \le r \le \rho, \qquad t_b \le t \le t_c. \tag{A.46}$$

The upper limit of the interval of applicability of these last two equations is $t_c$, rather than $t_{max}$, as will be explained in the next section.

In summary, for the interval $t_b \leq t \leq t_{max}$, the hinge-circle radius is found from Eq. A.34, and the plate velocity and displacement are given by Eqs. A.45 and A.46, respectively, in the interior of the hinge band and by Eqs. A.40 and A.41 in the exterior region. Performing the required differentiation on either side of the hinge circle, we can show that discontinuity conditions A.11 are satisfied; in fact, all the derivatives appearing in Eqs. A.11 are continuous at the hinge circle. Properly speaking, $\rho(t)$ should be referred to as a plastic regime boundary in the interval $t_b \leq t \leq t_{max}$, since the term "hinge circle" implies a discontinuity in $\partial V/\partial r$ at $\rho$. However, such a discontinuity occurs for $t_{max} \leq t \leq t_c$ so that $\rho$ is both a hinge circle and a regime boundary in the latter interval. Consequently, there seems little point in making the distinction in terminology.

Since $\beta(0) = t_b$, we have from Eqs. A.45 and A.46 that the velocity and displacement at the center of the plate are given by

$$\mu V_0(t) = \int_{t_b}^{t} P(\tau)\, d\tau + 2 \int_{t_y}^{t_b} [P(\tau) - P_y]\, d\tau,$$

$$\mu W_0(t) = \int_{t_b}^{t} (t - \tau)\, P(\tau)\, d\tau + 2 \int_{t_y}^{t_b} (t - \tau)[P(\tau) - P_y]\, d\tau,$$

$$t_b \leq t \leq t_c. \qquad \text{(A.47)}$$

c. Interval $t_{max} \leq t \leq t_c$

Equations A.24-A.33 remain applicable for this time interval. However, making the assumption that $\rho(t)$ is still given by Eq. A.34 would produce results which would violate discontinuity conditions A.11. Since $\rho(t)$ now starts to move back toward the origin, the function $\Omega(r)$ is known for every position $r \leq \rho$ that occurs during this time interval. Consequently, Eqs. A.45 and A.46 are still valid for the velocity and displacement inside the hinge band, as are Eqs. A.47 for the central velocity and displacement. We must still determine $\rho(t)$ and the velocity and displacement outside the hinge band.

Letting $r = \rho$ in Eq. A.45, we can write

$$\frac{\mu V_\rho(t)}{R-\rho} = \frac{1}{R-\rho}\int_{\beta(\rho)}^{t} P(\tau)\,d\tau + \int_{t_b}^{\beta(\rho)} \frac{P(\tau)}{R-\rho(\tau)}\,d\tau$$

$$+ \frac{2}{R}\int_{t_y}^{t_b} [P(\tau) - P_y]\,d\tau, \qquad t_{max} \le t \le t_c. \tag{A.48}$$

Differentiating Eq. A.48 with respect to time gives

$$\mu \frac{d}{dt}\left(\frac{V_\rho}{R-\rho}\right) = \frac{d\rho}{dt}\,\frac{1}{(R-\rho)^2}\int_{\beta(\rho)}^{t} P(\tau)\,d\tau$$

$$+ \frac{1}{(R-\rho)}\left[P(t) - P(\beta(\rho))\,\frac{d\beta}{d\rho}\,\frac{d\rho}{dt}\right]$$

$$+ \frac{P(\beta(\rho))}{R-\rho(\beta(\rho))}\,\frac{d\beta}{d\rho}\,\frac{d\rho}{dt}. \tag{A.49}$$

From Eqs. A.42 and A.43, we have

$$P(\beta(\rho)) = \frac{2P_y R^3}{(R+\rho)(R-\rho)^2}, \qquad \rho(\beta)\rho)) = \rho, \tag{A.50}$$

so that Eq. A.49 becomes

$$\mu \frac{d}{dt}\left(\frac{V_\rho}{R-\rho}\right) = \frac{d\rho}{dt}\,\frac{1}{(R-\rho)^2}\int_{\beta(\rho)}^{t} P(\tau)\,d\tau + \frac{P(t)}{R-\rho}. \tag{A.51}$$

Eliminating $(d/dt)[V_\rho/(R-\rho)]$ between Eqs. A.31b and A.51 then gives a differential equation for $\rho$; this equation is, after some algebraic manipulation,

$$\frac{d\rho}{dt}(R-\rho)(R+3\rho)\int_{\beta(\rho)}^{t} P(\tau)\,d\tau - P(t)(R+\rho)(R-\rho)^2 + 2P_y R^3 = 0. \tag{A.52}$$

Observing that

$$\frac{d}{d\rho}\left[(R+\rho)(R-\rho)^2\right] = -(R-\rho)(R+3\rho), \tag{A.53}$$

we are led to the identity

$$\frac{d}{dt}\left[(R+\rho)(R-\rho)^2\int_{\beta(\rho)}^{t} P(\tau)\,d\tau\right] = -\frac{d\rho}{dt}(R-\rho)(R+3\rho)\int_{\beta(\rho)}^{t} P(\tau)\,d\tau$$

$$+P(t)(R+\rho)(R-\rho)^2 - 2P_y R^3 \frac{d\beta}{d\rho}\frac{d\rho}{dt}, \tag{A.54}$$

where Eq. A.50 has been used. Differential equation A.52 can then be rewritten, using Eq. A.54, as

$$-\frac{d}{dt}\left[(R+\rho)(R-\rho)^2\int_{\beta(\rho)}^{t} P(\tau)\,d\tau\right] + 2P_y R^3\left[1 - \frac{d\beta}{d\rho}\frac{d\rho}{dt}\right] = 0. \tag{A.55}$$

The integration of Eq. A.55 gives

$$-(R+\rho)(R-\rho)^2\int_{\beta(\rho)}^{t} P(\tau)\,d\tau + 2P_y R^3[t-\beta(\rho)] + C_3 = 0, \tag{A.56}$$

where $C_3$ is an arbitrary constant. At $t = t_{max}$, $\rho = \rho_{max}$ and, from Eq. A.42, $\beta(\rho_{max}) = t_{max}$; consequently,

$$C_3 = 0. \tag{A.57}$$

The equation that determines $\rho(t)$ is therefore

$$\int_{\beta(\rho)}^{t} P(\tau)\,d\tau = \frac{2P_y R^3[t-\beta(\rho)]}{(R+\rho)(R-\rho)^2}, \qquad t_{max} \le t \le t_c. \tag{A.58}$$

The hinge circle motion ceases at $t_c$ when $\rho = 0$. Since, by Eq. 42, $\beta(0) = t_b$, the time $t_c$ is found from Eq. A.58 to be determined by solving

$$\int_{t_b}^{t_c} P(t)\,dt = 2P_y(t_c - t_b), \tag{A.59}$$

or, using Eq. A.19,

$$\int_{t_b}^{t_c} P(t)\, dt = P_b(t_c - t_b). \tag{A.60}$$

The last equation has the interpretation that the average pressure over the interval when the hinge band exists is the pressure at which the band is initiated.

The velocity distribution outside the hinge-band region will be found next. From Eqs. A.29 and A.48, we have

$$\mu V(r,t) = \frac{R - r}{R - \rho} \int_{\beta(\rho)}^{t} P(\tau)\, d\tau + (R - r) \int_{t_b}^{\beta(\rho)} \left( \frac{P(\tau)}{R - \rho(\tau)} \right) d\tau$$

$$+ \frac{2(R - r)}{R} \int_{t_y}^{t_b} [P(\tau) - P_y]\, d\tau,$$

$$\rho(t) \le r \le R, \qquad t_{max} \le t \le t_c. \tag{A.61}$$

This expression is inconvenient to use in determining the displacement in the region. Alternatively, we can write

$$V(r,t) = \int_{t_{max}}^{t} \frac{\partial V(r,\tau)}{\partial \tau}\, d\tau + V(r,t_{max}), \tag{A.62}$$

which, using Eq. A.29, becomes

$$V(r,t) = (R - r) \int_{t_{max}}^{t} \frac{d}{d\tau} \left( \frac{V_\rho}{R - \rho} \right) d\tau + V(r,t_{max}). \tag{A.63}$$

The integrand is given in Eq. A.31b, while $V(r,t_{max})$ is found from Eq. A.40. An alternate equation for the velocity is therefore

$$\mu V(r,t) = (R - r) \left[ \int_{t_{max}}^{t} H(\tau)\, d\tau + \frac{2}{R} \int_{t_y}^{t_b} [P(\tau) - P_y]\, d\tau \right.$$

$$\left. + \int_{t_b}^{t_{max}} \frac{P(\tau)}{R - \rho(\tau)}\, d\tau \right], \qquad \rho(t) \le r \le R, \qquad t_{max} \le t \le t_c, \tag{A.64}$$

where

$$H(t) = \frac{2}{(R-\rho)(R+3\rho)}\left[(R+2\rho)\,P - \frac{R^3 P_y}{(R-\rho)^2}\right], \qquad t_{max} \le t \le t_c. \tag{A.65}$$

The displacement in the region $\rho(t) \le r \le \rho_{max}$ can be written

$$W(r,t) = \int_{t_{max}}^{t_r} V(r,\tau)\,d\tau + \int_{t_r}^{t} V(r,\tau)\,d\tau + W(r,t_{max}), \tag{A.66}$$

where $t = t_r$ when $\rho(t) = r$. By Eq. A.58, $t_r$ is found from

$$\int_{\beta(r)}^{t_r} P(\tau)\,d\tau = \frac{2P_y R^3[t_r - \beta(r)]}{(R+r)(R-r)^2}. \tag{A.67}$$

In the first integral of Eq. A.66, $r < \rho$, so that V is given by Eq. A.45; while in the second integral, $r > \rho$, so that V is given by Eq. A.64. Making the substitutions for V, performing integrations by parts, evaluating Eq. A.46 at $t_{max}$, and using Eqs. A.65, A.31b, and A.48 lead to

$$\mu W(r,t) = (R-r)\left\{\int_{t_r}^{t} (t-\tau)\,H(\tau)\,d\tau + \int_{t_b}^{\beta(r)} \frac{(t-\tau)\,P(\tau)}{R-\rho(\tau)}\,d\tau \right.$$

$$\left. + \frac{2}{R}\int_{t_y}^{t_b} (t-\tau)[P(\tau) - P_y]\,d\tau\right\} + \int_{\beta(r)}^{t_r} (t-\tau)\,P(\tau)\,d\tau,$$

$$\rho(t) \le r \le \rho_{max}, \qquad t_{max} \le t \le t_c. \tag{A.68}$$

The displacement in the region $\rho_{max} \le r \le R$ can be written

$$W(r,t) = \int_{t_{max}}^{t} V(r,\tau)\,d\tau + W(r,t_{max}). \tag{A.69}$$

In the integral, $r > \rho$, so that V is given by Eq. A.64. Making this substitution, evaluating W at $t_{max}$ from Eq. A.41, and performing some integrations by parts, we arrive at

$$\mu W(r,t) = (R - r)\left\{\int_{t_{max}}^{t} (t - \tau)\, H(\tau)\, d\tau + \int_{t_b}^{t_{max}} \frac{(t - \tau)\, P(\tau)}{R - \rho(\tau)}\, d\tau \right.$$

$$\left. + \frac{2}{R} \int_{t_y}^{t_b} (t - \tau)[P(\tau) - P_y]\, d\tau \right\}$$

$$\rho_{max} \le r \le R, \qquad t_{max} \le t \le t_c. \tag{A.70}$$

Discontinuity conditions A.11 are satisfied in the interval $t_{max} \le t \le t_c$ for $V(r,t)$ given by Eqs. A.45 and A.64, $W(r,t)$ given by Eqs. A.46 and A.68, and $\rho(t)$ given by Eq. A.58. Unlike the previous interval, a discontinuity in $\partial V/\partial r$ occurs at $\rho$, so $\rho$ is properly called a hinge circle. From Eqs. A.31c and A.52, we have that

$$\left.\frac{\partial^2 M_r}{\partial r^2}\right|_{r=\rho^+} = \frac{1}{R - \rho} \frac{d\rho}{dt} \int_{\beta(\rho)}^{t} P\, d\tau. \tag{A.71}$$

Since $\rho$ decreases in this time interval and the integral is nonnegative, inequality A.32 holds and the yield condition is not violated in the region $\rho \le r \le R$.

The velocity and displacement distributions at $t_c$ are, using Eqs. A.61, A.68, A.70, and A.60,

$$\mu V(r,t_c) = \frac{2(R - r)}{R} \int_{t_y}^{t_c} [P(\tau) - P_y]\, d\tau, \qquad 0 \le r \le R,$$

$$\mu W(r,t_c) = (R - r)\left\{\int_{t_r}^{t_c} (t_c - \tau)\, H(\tau)\, d\tau + \int_{t_b}^{\beta(r)} \frac{(t_c - \tau)\, P(\tau)}{R - \rho(\tau)}\, d\tau \right.$$

$$\left. + \frac{2}{R} \int_{t_y}^{t_b} (t_c - \tau)[P(\tau) - P_y]\, d\tau \right\}$$

$$+ \int_{\beta(r)}^{t_r} (t_c - \tau)\, P(\tau)\, d\tau, \qquad 0 \le r \le \rho_{max}, \tag{A.72 (Contd.)}$$

$$\mu W(r,t_c) = (R - r)\left\{\int_{t_{max}}^{t_c} (t_c - \tau)\, H(\tau)\, d\tau + \int_{t_b}^{t_{max}} \frac{(t_c - \tau)\, P(\tau)}{R - \rho(\tau)}\, d\tau \right.$$

$$\left. + \frac{2}{R}\int_{t_y}^{t_b} (t_c - \tau)[P(\tau) - P_y]\, d\tau\right\}, \qquad \rho_{max} \le r \le R. \qquad \text{(Contd.)} \quad \text{(A.72)}$$

In particular, at $r = 0$, where $t_r = t_c$ and $\beta(r) = t_b$, we have

$$\mu V_0(t_c) = 2\int_{t_y}^{t_c} [P(\tau) - P_y]\, d\tau, \qquad \text{(A.73a)}$$

and

$$\mu W_0(t_c) = \int_{t_b}^{t_c} (t_c - \tau)\, P(\tau)\, d\tau + 2\int_{t_y}^{t_b} (t_c - \tau)[P(\tau) - P_y]\, d\tau. \qquad \text{(A.73b)}$$

d. Interval $t_c \le t \le t_f$

Since the hinge band has disappeared, Eqs. A.12, A.14b, and A.14c apply in this interval as they did in the initial interval $t_y \le t \le t_b$. After performing straightforward integrations with respect to time, we have, using Eq. A.73a,

$$\mu V(r,t) = \frac{2(R - r)}{R}\int_{t_y}^{t} [P(\tau) - P_y]\, d\tau, \qquad \text{(A.74a)}$$

$$\mu W(r,t) = \frac{2(R - r)}{R}\left\{\int_{t_y}^{t} (t - \tau)[P(\tau) - P_y]\, d\tau \right.$$

$$\left. - \int_{t_y}^{t_c} (t_c - \tau)[P(\tau) - P_y]\, d\tau\right\} + \mu W(r,t_c),$$

$$0 \le r \le R, \qquad t_c \le t \le t_f. \qquad \text{(A.74b)}$$

In particular,

$$\mu V_0(t) = 2 \int_{t_y}^{t} [P(\tau) - P_y]\, d\tau, \tag{A.75a}$$

$$\mu W_0(t) = 2 \int_{t_y}^{t} (t - \tau)[P(\tau) - P_y]\, d\tau - 2 \int_{t_b}^{t_c} (t_c - \tau)[P(\tau) - P_y]\, d\tau$$

$$+ \int_{t_b}^{t_c} (t_c - \tau)\, P(\tau)\, d\tau, \qquad t_c \le t \le t_f. \tag{A.75b}$$

The time $t_f$ is when the plate deformation ceases; from Eq. A.74a, this is determined from

$$\int_{t_y}^{t_f} P(t)\, dt = P_y(t_f - t_y), \tag{A.76}$$

which is identical to Eq. A.21. This equation has the interpretation that the average pressure during the deformation is the yield pressure.

Evaluating $W_0(t_f)$ from Eq. A.75b, using Eqs. A.60 and A.76, we have, after some algebraic rearrangement,

$$\mu W_0(t_f) = \frac{1}{P_y} \left[ \int_{t_y}^{t_f} P(t)\, dt \right]^2 - \frac{1}{4P_y} \left[ \int_{t_b}^{t_c} P(t)\, dt \right]^2$$

$$- 2 \int_{t_y}^{t_f} (t - t_y)\, P(t)\, dt + \int_{t_b}^{t_c} (t - t_b)\, P(t)\, dt. \tag{A.77}$$

Define $I^*$, $t^*_{mean}$, and $P^*_e$ by

$$\left.\begin{aligned} I^* &= \int_{t_b}^{t_c} P(t)\, dt, \\ t^*_{mean} &= \frac{1}{I^*} \int_{t_b}^{t_c} (t - t_b)\, P(t)\, dt, \end{aligned}\right\} \tag{A.78 (Contd.)}$$

and

$$P_e^* = \frac{I^*}{2t^*_{mean}}. \qquad \text{(Contd.) (A.78)}$$

Then, from Eqs. A.77, A.78, and A.22, we have

$$W_0(t_f) = \frac{I^2}{\mu P_y}\left[1 - \frac{P_y}{P_e} - \frac{1}{2}\left(\frac{I^*}{I}\right)^2\left(\frac{1}{2} - \frac{P_y}{P_e^*}\right)\right]. \qquad \text{(A.79)}$$

5. Rectangular Pulse

The solution of Hopkins and Prager[4] for a rectangular pulse can be derived as a special case of the general solution obtained here. Let P(t) be given by

$$\left.\begin{aligned} P(t) &= P_{max}, \quad 0 \le t \le t_0, \\ &= 0, \quad t > t_0. \end{aligned}\right\} \qquad \text{(A.80)}$$

Then,

$$\left.\begin{aligned} t_y &= t_b = t_{max} = \beta(\rho) = 0, \\ I &= I^* = P_{max}\, t_0, \\ P_e &= P_e^* = P_{max}, \\ t_f &= \frac{P_{max}}{P_y}\, t_0, \quad P_{max} > P_y, \end{aligned}\right\} \qquad \text{(A.81)}$$

and

$$t_c = \frac{P_{max}}{2P_y}\, t_0, \quad P_{max} > 2P_y.$$

a. Load Range $P_y < P_{max} < 2P_y$

The radial bending moment as given by Eq. A.14c becomes

$$\left.\begin{aligned} \frac{M_r}{M_0} &= \left(1 - \frac{r}{R}\right)\left(\frac{P_{max}}{P_y}\,\frac{r^2}{R^2} + 1 + \frac{r}{R} - \frac{r^2}{R^2}\right), \quad 0 \le t \le t_0, \\ \frac{M_r}{M_0} &= 1 - 2\,\frac{r^2}{R^2} + \frac{r^3}{R^3}, \quad t_0 < t < t_f. \end{aligned}\right\} \qquad \text{(A.82)}$$

The velocity and displacement are found from Eqs. A.12 and A.16 to be

$$\left.\begin{aligned} V(r,t) &= \frac{2(R-r)}{\mu R}(P_{max}-P_y)\,t, \qquad 0 \le t \le t_0, \\ V(r,t) &= \frac{2(R-r)}{\mu R}(P_{max}t_0 - P_y t), \qquad t_0 < t \le t_f, \\ W(r,t) &= \frac{R-r}{\mu R}(P_{max}-P_y)\,t^2, \qquad 0 \le t \le t_0, \end{aligned}\right\} \tag{A.83}$$

and

$$\left.\begin{aligned} W(r,t) &= \frac{R-r}{\mu R}[P_{max}t_0(2t-t_0) - P_y t^2], \qquad t_0 < t \le t_f, \end{aligned}\right\}$$

and the final displacement at the plate center is found from Eq. A.23 to be

$$W_0(t_f) = \frac{P_{max}^2 t_0^2}{\mu P_y}\left(1 - \frac{P_y}{P_{max}}\right). \tag{A.84}$$

b. Load Range $P_{max} \ge 2P_y$

At $t = 0$, a hinge band forms instantaneously in the region $0 \le r \le \rho_{max}$. By Eq. A.34, $\rho_{max}$ is found from

$$(R+\rho_{max})(R-\rho_{max})^2 = \frac{2P_y R^3}{P_{max}}. \tag{A.85}$$

For $0 \le t \le t_c$, $\rho(t)$ is determined from Eq. A.58 to be given by

$$\left.\begin{aligned} \rho(t) &= \rho_{max}, \qquad 0 \le t \le t_0, \end{aligned}\right\}$$

and

$$\left.\begin{aligned} (R+\rho)(R-\rho)^2 &= \frac{2P_y R^3 t}{P_{max}t_0}, \qquad t_0 \le t \le t_c. \end{aligned}\right\} \tag{A.86}$$

From Eqs. A.31c and A.86, we have for the radial bending moment in the region $\rho \le r \le R$

$$\left.\begin{aligned} \frac{M_r}{M_0} &= 1 - \frac{R(r+\rho_{max})(r-\rho_{max})^3}{r(R+\rho_{max})(R-\rho_{max})^3}, \qquad 0 \le t \le t_0, \end{aligned}\right\} \tag{A.87}$$

(Contd.)

and

$$\frac{M_r}{M_0} = \frac{(R - r)(R^3r + R^2r^2 - Rr^3 - 4R\rho^3 + 3\rho^4)}{r(R + 3\rho)(R - \rho)^3}, \qquad t_0 < t \le t_c. \qquad \text{(Contd.) (A.87)}$$

For $0 \le r \le \rho$, the velocity and displacement are given by Eq. A.45 and A.46 to be

$$\left.\begin{aligned} V(r,t) &= \frac{P_{max}t}{\mu}, \qquad 0 \le t \le t_0, \\ V(r,t) &= \frac{P_{max}t_0}{\mu}, \qquad t_0 \le t \le t_c, \\ W(r,t) &= \frac{P_{max}t^2}{2\mu}, \qquad 0 \le t \le t_0, \end{aligned}\right\} \qquad \text{(A.88)}$$

and

$$\left.\begin{aligned} W(r,t) &= \frac{P_{max}t_0(2t - t_0)}{2\mu}, \qquad t_0 \le t \le t_c, \end{aligned}\right\}$$

while outside the hinge band ($\rho \le r \le R$), from Eqs. A.61, A.68, and A.70,

$$\left.\begin{aligned} V(r,t) &= \frac{R - r}{R - \rho_{max}} \frac{P_{max}t}{\mu}, \qquad 0 \le t \le t_0, \\ V(r,t) &= \frac{R - r}{R - \rho(t)} \frac{P_{max}t_0}{\mu}, \qquad t_0 \le t \le t_c, \\ W(r,t) &= \frac{R - r}{R - \rho_{max}} \frac{P_{max}t^2}{2\mu}, \qquad 0 \le t \le t_0, \\ W(r,t) &= \frac{P_{max}t_0^2}{2\mu} \left\{ \frac{(R - r)[(R + \rho)(R - 3\rho) + (R + r)^2]}{(R + \rho_{max})(R - \rho_{max})^2} - 1 \right\}, \\ & \rho \le r \le \rho_{max}, \qquad t_0 \le t \le t_c, \end{aligned}\right\} \qquad \text{(A.89)}$$

and

$$\left.\begin{aligned} W(r,t) &= \frac{P_{max}t_0^2(R - r)}{2\mu} \left[ \frac{2\rho_{max}(R + \rho_{max}) + (R + \rho)(R - 3\rho)}{(R + \rho_{max})(R - \rho_{max})^2} \right], \\ & \rho_{max} \le r \le R, \qquad t_0 \le t \le t_c. \end{aligned}\right\}$$

In particular,

$$\left.\begin{aligned} V(r,t_c) &= \frac{R-r}{\mu R} P_{max} t_0, \\ W(r,t_c) &= \frac{P_{max} t_0^2}{2\mu} \left[ \frac{P_{max}}{2P_y} \left( 2 - \frac{r^2}{R^2} - \frac{r^3}{R^3} \right) - 1 \right], \quad 0 \le r \le \rho_{max}, \end{aligned}\right\} \tag{A.90}$$

and

$$W(r,t_c) = \frac{P_{max} t_0^2}{2\mu} (R-r) \left[ \frac{(R+\rho_{max})^2 + \rho_{max}^2}{(R+\rho_{max})(R-\rho_{max})^2} \right], \quad \rho_{max} \le r \le R.$$

For $t_c \le t \le t_f$, Eqs. A.14c and A.74 give

$$\left.\begin{aligned} \frac{M_r}{M_0} &= \frac{R-r}{R} \left( 1 + \frac{r}{R} - \frac{r^2}{R^2} \right), \\ V(r,t) &= \frac{2(R-r)}{\mu R} (P_{max} t_0 - P_y t), \end{aligned}\right\} \tag{A.91}$$

and

$$W(r,t) = \frac{R-r}{\mu R} [2P_{max} t_0 - P_y (t + t_c)](t - t_c) + W(r,t_c).$$

In particular,

$$\left.\begin{aligned} W(r,t_f) &= \frac{P_{max} t_0^2}{2\mu} \left[ \frac{P_{max}}{2P_y} \left( 3 - \frac{r}{R} - \frac{r^2}{R^2} - \frac{r^3}{R^3} \right) - 1 \right], \quad 0 \le r \le \rho_{max}, \\ W(r,t_f) &= \frac{P_{max}^2 t_0^2}{2\mu P_y} \left( 1 - \frac{r}{R} \right) \left( 1 + \frac{\rho_{max}}{R} + \frac{\rho_{max}^2}{R^2} \right), \quad \rho_{max} \le r \le R, \end{aligned}\right\} \tag{A.92}$$

and

$$W(0,t_f) = \frac{P_{max}^2 t_0^2}{2\mu P_y} \left( \frac{3}{2} - \frac{P_y}{P_{max}} \right).$$

The equations of this section are the same as those obtained by Hopkins and Prager except for the expressions for $W(r,t)$ for $t_0 < t < t_f$ which are not given in Ref. 4.

## 6. Pulse That Attains Its Maximum Instantaneously

Perzyna[3] treats loads characterized by

$$\int_0^t P(\tau)\, d\tau \geq tP(t), \tag{A.93}$$

i.e., the pressure attains its maximum instantaneously and decays thereafter. He refers to these loads as "blast" loads and calls the general loading of Fig. 1a an "impact" load. His results can be obtained from the "impact"-load solution derived here by taking

$$t_y = t_b = t_{max} = \beta(\rho) = 0, \tag{A.94}$$

which eliminates many of the integrals in the expressions for the velocity and displacement. Perzyna solved differential equation A.52 numerically for the hinge motion for two particular load shapes and did not obtain the general closed-form solution Eq. A.58.

## APPENDIX B

## Solution for Reinforced Circular Cylindrical Shell for General Pulse Shape

### 1. Introduction

The dynamic plastic deformation of a rigidly reinforced,* circular cylindrical shell subjected to a uniform pressure is treated by Hodge.[2] He obtains closed-form solutions for pressure pulses that rise instantaneously to their maximum and then decay monotonically and also for more general pulse shapes if no hinge-band formation occurs. His analysis will be extended in this appendix to include the case of the general pulse shape of Fig. 14 where a hinge band is produced. The method of solution is the same as that used in the analysis for the circular plate in Appendix A.

### 2. Statement of Problem

Consider the reinforced circular cylindrical shell of Fig. 2b having radius A, thickness H, distance 2L between reinforcements, and surface density $\mu$. The usual shell-theory assumptions are made so that stress distributions across the shell thickness are replaced by their resultant direct stresses, bending moments, and shears. Assume that the shell material is rigid, perfectly plastic, with yield stress $\sigma_Y$. The problem can be formulated in terms of only two resultants: the circumferential stress resultant $N_\phi$ and the axial bending moment resultant $M_r$. The equation of motion is

$$\frac{\partial^2 M_z}{\partial z^2} + \frac{N_\phi}{A} + P = \mu \frac{\partial^2 W}{\partial t^2}, \tag{B.1}$$

where z is axial position, t is time, P(t) is the applied external pressure, and W(z,t) is the radial displacement, considered positive inward. Only the typical half-bay $0 \leq z \leq L$ need be considered.

The yield condition is taken to be the limited interaction condition of Fig. 3b, i.e., a rectangle with vertices $(\pm M_0, \pm N_0)$, where

$$M_0 = \tfrac{1}{4} \sigma_Y H^2, \qquad N_0 = \sigma_Y H. \tag{B.2}$$

The flow rule states that the flow vector, with components proportional to $-\partial^2 V/\partial z^2$ and $-V$, where V is the radial velocity, is in the direction of the outward perpendicular to the yield locus at the yield state $(M_z, N_\phi)$.

*Nonrigid reinforcements are treated by Nemirovsky and Mazalov.[10]

The three plastic regimes occurring in this problem are:

$$\text{Regime A: } M_z = -M_0,\ N_\phi = -N_0,\ \frac{\partial^2 V}{\partial z^2} \geq 0,\ V \geq 0; \tag{B.3a}$$

$$\text{Regime AB: } -M_0 < M_z < M_0,\ N_\phi = -N_0,\ \frac{\partial^2 V}{\partial z^2} = 0,\ V \geq 0; \tag{B.3b}$$

$$\text{Regime B: } M_z = M_0,\ N_\phi = -N_0,\ \frac{\partial^2 V}{\partial z^2} \leq 0,\ V \geq 0. \tag{B.3c}$$

During the entire cylinder deformation,

$$N_\phi = -N_0, \quad 0 \leq z \leq L. \tag{B.4}$$

At the rigid reinforcement, the cylinder is in Regime A and

$$V = W = 0, \tag{B.5a}$$

$$M_z = -M_0, \text{ at } z = 0. \tag{B.5b}$$

When there is no hinge band, the center of the unsupported span is in Regime B; moreover, because of symmetry, there is no shear force. The boundary conditions are, consequently,

$$\left.\begin{aligned} &M_z = M_0, \\ &\text{and} \\ &\frac{\partial M_z}{\partial z} = 0 \text{ at } z = L. \end{aligned}\right\} \tag{B.6}$$

The remainder of the half-span is in Regime AB, so that

$$-M_0 < M_z < M_0,\ \frac{\partial^2 V}{\partial z^2} = 0,\ V \geq 0 \text{ for } 0 < z < L. \tag{B.7}$$

If a hinge band appears in the region $\zeta(t) \leq z \leq L$, the entire band is in Regime B; therefore,

$$M_z = M_0,\ \frac{\partial M_z}{\partial z} = 0,\ \frac{\partial^2 V}{\partial z^2} \leq 0,\ V \geq 0 \text{ for } \zeta \leq z \leq L. \tag{B.8}$$

In the remainder of the half-span, which is still in Regime AB,

$$-M_0 < M_z < M_0, \quad \frac{\partial^2 V}{\partial z^2} = 0, \quad V \geq 0 \text{ for } 0 < z < \zeta. \tag{B.9}$$

The initial conditions of the cylinder motion are

$$V(z,t_y) = W(z,t_y) = 0, \tag{B.10}$$

where $t_y$ is the time when the yield pressure is first attained.

If no hinge band occurs, we must solve differential equation B.1 subject to initial conditions B.10 and boundary conditions and restrictions B.4-B.7. If there is a hinge band, conditions B.6 and B.7 are replaced by B.8 and B.9.

The conditions on permissible discontinuities at the hinge circle $\zeta(t)$ are similar to those given for the circular plate and will not be discussed here.

3. Solution for $P_{max} \leq P_b$

From the limit-load analysis,[2] the yield pressure $P_y$ is

$$P_y = P_0 \left(1 + \frac{AH}{L^2}\right), \tag{B.11}$$

where

$$P_0 = \frac{\sigma_y H}{A}. \tag{B.12}$$

Take

$$V(z,t) = V_L(t)\frac{z}{L}, \tag{B.13}$$

where $V_L$ is the inward radial velocity at the midpoint of the span; V then meets the requirements stated in Eqs. B.5a and B.7. The integration of differential equation B.1 twice with respect to z gives, using Eqs. B.13, B.4, B.12, and B.2,

$$M_z(z,t) = [P_0 - P(t)]\frac{z^2}{2} + \frac{\mu z^3}{6L}\frac{dV_L}{dt} + C_1(t)z + C_2(t). \tag{B.14}$$

Applying boundary conditions B.5b and B.6 results in

$$C_2 = -\tfrac{1}{4}(P_y - P_0)L^2, \tag{B.15a}$$

$$C_1 = \frac{L}{4}\,[P - P_0 + 3(P_y - P_0)], \tag{B.15b}$$

$$\frac{dV_L}{dt} = \frac{3(P - P_y)}{2\mu}, \tag{B.15c}$$

and

$$M_z = \frac{1}{4L}\,(P - P_0)\,z(L - z)^2 + \frac{1}{4L}\,(P_y - P_0)(-L^3 + 3zL^2 - z^3). \tag{B.15d}$$

The solution to differential equation B.15c is, using Eqs. B.10 and B.13,

$$V_L(t) = \frac{3}{2\mu}\int_{t_y}^{t} [P(\tau) - P_y]\,d\tau. \tag{B.16}$$

Integrating Eq. B.16 with respect to time, we obtain

$$\left.\begin{aligned} W_L(t) &= \frac{3}{2\mu}\int_{t_y}^{t} (t - \tau)[P(\tau) - P_y]\,d\tau \\ \text{and} \\ W(z,t) &= \frac{z}{L}\,W_L(t), \end{aligned}\right\}, \tag{B.17}$$

where $W_L$ is the displacement at $z = L$.

Since $M_z$ is a cubic in $z$ and Eqs. B.5b and B.6 are satisfied, the condition that $|M_z| \leq M_0$ in the region $0 < z < L$ is equivalent to requiring

$$\frac{\partial M_z}{\partial z} > 0 \text{ at } z = 0 \tag{B.18}$$

and

$$\frac{\partial^2 M_z}{\partial z^2} < 0 \text{ at } z = L. \tag{B.19}$$

From Eq. B.15d, inequality B.18 implies

$$P(t) > 4P_0 - 3P_y, \tag{B.20}$$

which by Eqs. B.11 and B.12 means

$$L^2 < 3AH. \tag{B.21}$$

As in Ref. 2, it will be assumed that the problem configuration is such that inequality B.21 is satisfied. Inequality B.19 is equivalent to, using Eq. B.15d,

$$P(t) < 3P_y - 2P_0. \tag{B.22}$$

Define

$$P_b = 3P_y - 2P_0 \tag{B.23}$$

as the load at which a hinge band is initiated at $z = L$. The condition that $P(t)$ does not produce a hinge band is then

$$P_{max} \leq P_b. \tag{B.24}$$

The plastic deformation ends at time $t_f$ when the velocity vanishes. From Eq. B.16, $t_f$ is found from

$$\int_{t_y}^{t_f} P(\tau)\, d\tau = P_y(t_f - t_y). \tag{B.25}$$

Using definitions A.22 for I and $P_e$, we then obtain the final plastic deformation from Eqs. B.17 and B.25 as

$$W(z,t_f) = \frac{3I^2}{4\mu P_y}\left(1 - \frac{P_y}{P_e}\right)\frac{z}{L}$$

and

$$W_L(t_f) = \frac{3I^2}{4\mu P_y}\left(1 - \frac{P_y}{P_e}\right). \tag{B.26}$$

4. Solution for $P_{max} > P_b$

a. Interval $t_y \leq t \leq t_b$

The solution given by Eqs. B.13-B.17 is applicable up to time $t_b$ when the pressure first reaches $P_b$ and $\partial^2 M_z/\partial z^2 = 0$ at $z = L$. At this time, a hinge circle $\zeta(t)$ separating the region of the cylinder in Regime B from the region in Regime AB begins to move out from $z = L$.

b. Interval $t_b \leq t \leq t_{max}$

Consider first the hinge-band region where $M_z = M_0$. Differential equation B.1 becomes

$$\mu \frac{\partial V}{\partial t} = P - P_0. \tag{B.27}$$

The solution of Eq. B.27 is

$$\mu V(z,t) = \int_{t_b}^{t} [P(\tau) - P_0]\, d\tau + \Omega(z), \qquad \zeta \leq z \leq L, \tag{B.28}$$

where $\Omega(z)$ is determined from the continuity of the velocity at the edge of the band. Letting

$$V_\zeta(t) = V(\zeta(t),t), \tag{B.29}$$

$\Omega$ is found from

$$\Omega(\zeta) = \mu V_\zeta - \int_{t_b}^{t} [P(\tau) - P_0]\, d\tau, \tag{B.30}$$

where t is viewed as a function of $\zeta$ rather than the converse.

In the region $0 \leq z \leq \zeta$, take

$$V(z,t) = V_\zeta(t) \frac{z}{\zeta(t)}. \tag{B.31}$$

The double integration of Eq. B.1 with respect to z results in

$$M_z = (P_0 - P) \frac{z^2}{2} + \frac{\mu z^3}{6} \frac{d}{dt} \left( \frac{V_\zeta}{\zeta} \right) + C_3(t)z + C_4(t). \tag{B.32}$$

Applying boundary condition B.5b at $z = 0$ and the continuity requirements that

$$M_z = M_0, \quad \frac{\partial M_z}{\partial z} = 0 \text{ at } z = \zeta, \tag{B.33}$$

we arrive at

$$C_4 = -\frac{1}{4}(P_y - P_0) L^2, \tag{B.34a}$$

$$C_3 = \frac{1}{4\zeta}[(P - P_0)\zeta^2 + 3(P_y - P_0) L^2], \tag{B.34b}$$

$$\frac{d}{dt}\left(\frac{V_\zeta}{\zeta}\right) = \frac{3}{2\mu\zeta^3}[(P - P_0)\zeta^2 - (P_y - P_0) L^2], \tag{B.34c}$$

$$M_z = \frac{z}{4\zeta}(\zeta - z)^2(P - P_0) + \frac{L^2}{4\zeta^3}(-\zeta^3 + 3\zeta^2 z - z^3)(P_y - P_0),$$

$$0 \le z \le \zeta, \quad t_b \le t \le t_c. \tag{B.34d}$$

The condition that $M_z$ should not exceed $M_0$ in the vicinity of $z = \zeta$ requires that

$$\frac{\partial^2 M_z}{\partial z^2} \le 0 \text{ at } z = \zeta-. \tag{B.35}$$

Using Eq. B.34d this is equivalent to

$$(P - P_0)\zeta^2 \le 3(P_y - P_0) L^2, \quad t_b \le t \le t_c. \tag{B.36}$$

Following a similar line of reasoning to that employed in the circular plate problem, we will assume that the equality in Eq. B.36 holds while the pressure is increasing. The resulting solution can then be shown to satisfy all the requirements of the problem. Accordingly, we will take

$$\zeta(t) = L\sqrt{\frac{3(P_y - P_0)}{P(t) - P_0}}, \quad t_b \le t \le t_{max}, \tag{B.37a}$$

and

$$\zeta_{max} = L\sqrt{\frac{3(P_y - P_0)}{P_{max} - P_0}}. \tag{B.37b}$$

Using Eq. B.37a to simplify Eqs. B.34d and B.34c gives

$$\frac{M_z}{M_0} = 1 - 2\frac{(\zeta - z)^3}{\zeta^3}, \tag{B.38a}$$

and

$$\frac{d}{dt}\left(\frac{V_\zeta}{\zeta}\right) = \frac{1}{\mu L}\sqrt{\frac{(P - P_0)^3}{3(P_y - P_0)}}, \qquad t_b \le t \le t_{max}. \tag{B.38b}$$

Equation B.38b can be integrated to give

$$\frac{V_\zeta}{\zeta} = \frac{1}{\mu L\sqrt{3(P_y - P_0)}} \int_{t_b}^{t} [P(\tau) - P_0]^{3/2}\, d\tau + \frac{V_\zeta(t_b)}{\zeta(t_b)}. \tag{B.39}$$

Since $V_\zeta(t_b) = V_L(t_b)$ and $\zeta(t_b) = L$, we have from Eq. B.16 that

$$V_\zeta(t) = \frac{1}{\mu\sqrt{P(t) - P_0}} \left\{ \int_{t_b}^{t} [P(\tau) - P_0]^{3/2}\, d\tau \right.$$

$$\left. + \frac{3}{2}\sqrt{3(P_y - P_0)} \int_{t_y}^{t_b} [P(\tau) - P_y]\, d\tau \right\}, \tag{B.40}$$

so that, using Eqs. B.31 and B.37, we arrive at

$$V(z,t) = \frac{z}{\mu L} \left\{ \frac{1}{\sqrt{3(P_y - P_0)}} \int_{t_b}^{t} [P(\tau) - P_0]^{3/2}\, d\tau \right.$$

$$\left. + \frac{3}{2} \int_{t_y}^{t_b} [P(\tau) - P_y]\, d\tau \right\},$$

$$0 \le z \le \zeta, \qquad t_b \le t \le t_{max}. \tag{B.41}$$

The displacement is found by integrating the velocity from $t_b$ to t and making use of Eq. B.17 to calculate $W(z,t_b)$; the result is

$$W(z,t) = \frac{z}{\mu L}\left\{\frac{1}{\sqrt{3(P_y - P_0)}}\int_{t_b}^{t}(t-\tau)[P(\tau)-P_0]^{3/2}\,d\tau + \frac{3}{2}\int_{t_y}^{t_b}(t-\tau)[P(\tau)-P_y]\,d\tau\right\},$$

$$0 \le z \le \zeta, \qquad t_b \le t \le t_{max}. \tag{B.42}$$

The function $\Omega(z)$ can now be determined as follows: The function $\zeta(t)$ given in Eq. B.37a can be inverted to give

$$t = \beta(\zeta), \quad L \ge \zeta \ge \zeta_{max}, \quad t_b \le t \le t_{max}, \tag{B.43}$$

where

$$\beta(\zeta) = P^{-1}\left[P_0 + 3(P_y - P_0)\frac{L^2}{\zeta^2}\right], \qquad P_b \le P(t) \le P_{max}. \tag{B.44}$$

Substituting from Eqs. B.40 and B.43 into Eq. B.30, we arrive at

$$\Omega(\zeta) = \frac{\zeta}{L}\left\{\frac{1}{\sqrt{3(P_y - P_0)}}\int_{t_b}^{\beta(\zeta)}[P(\tau)-P_0]^{3/2}\,d\tau + \frac{3}{2}\int_{t_y}^{t_b}[P(\tau)-P_y]\,d\tau\right\} - \int_{t_b}^{\beta(\zeta)}[P(\tau)-P_0]\,d\tau, \qquad L \ge \zeta \ge \zeta_{max}. \tag{B.45}$$

Using this result in Eq. B.28 then gives

$$\mu V(z,t) = \int_{\beta(z)}^{t}[P(\tau)-P_0]\,d\tau + \frac{3z}{2L}\int_{t_y}^{t_b}[P(\tau)-P_y]\,d\tau + \frac{z}{L\sqrt{3(P_y - P_0)}}\int_{t_b}^{\beta(z)}[P(\tau)-P_0]^{3/2}\,d\tau,$$

$$\zeta \le z \le L, \qquad t_b \le t \le t_c. \tag{B.46}$$

Integrating the velocity from $t_b$ to t and using Eq. B.17 to find $W(z,t_b)$, we obtain

$$\mu W(z,t) = \int_{\beta(z)}^{t} (t-\tau)[P(\tau) - P_0]\, d\tau + \frac{3z}{2L} \int_{t_y}^{t_b} (t-\tau)[P(\tau) - P_y]\, d\tau$$

$$+ \frac{z}{L\sqrt{3(P_y - P_0)}} \int_{t_b}^{\beta(z)} (t-\tau)[P(\tau) - P_0]^{3/2}\, d\tau,$$

$$\zeta \le z \le L, \qquad t_b \le t \le t_c. \tag{B.47}$$

The upper limit of the interval of applicability of Eqs. B.46 and B.47 is $t_c$, rather than $t_{max}$, because the reversal of direction of the hinge-circle motion does not affect the velocity distribution, and hence the displacement equation, inside the hinge band.

As in the plate problem, all the functions appearing in the discontinuity relations are continuous at $\zeta$ in the interval $t_b \le t \le t_{max}$. Consequently, the solution obtained by making the assumption that Eq. B.37a holds is correct for this interval.

Since $\beta(L) = t_b$, we have from Eqs. B.46 and B.47 that the velocity and displacement at z = L are given by

$$\mu V_L(t) = \int_{t_b}^{t} [P(\tau) - P_0]\, d\tau + \frac{3}{2} \int_{t_y}^{t_b} [P(\tau) - P_y]\, d\tau,$$

$$\mu W_L(t) = \int_{t_b}^{t} (t-\tau)[P(\tau) - P_0]\, d\tau + \frac{3}{2} \int_{t_y}^{t_b} (t-\tau)[P(\tau) - P_y]\, d\tau,$$

$$t_b \le t \le t_c. \tag{B.48}$$

c. Interval $t_{max} \le t \le t_c$

Equations B.27-B.36 remain applicable for this time interval. However, making the assumption that $\zeta(t)$ is still given by Eq. B.37a would lead to results that would violate the discontinuity restrictions. Since the hinge circle now starts to move back toward z = L, it passes through previously occupied positions for which $\Omega(\zeta)$ is known. Consequently, Eqs. B.46-B.48 remain valid for the velocity and displacement inside the hinge band.

Putting $z = \zeta$ in Eq. B.46, we can write

$$\mu \frac{V_\zeta(t)}{\zeta(t)} = \frac{1}{\zeta} \int_{\beta(\zeta)}^{t} [P(\tau) - P_0]\, d\tau + \frac{3}{2L} \int_{t_y}^{t_b} [P(\tau) - P_y]\, d\tau$$

$$+ \frac{1}{L\sqrt{3(P_y - P_0)}} \int_{t_b}^{\beta(\zeta)} [P(\tau) - P_0]^{3/2}\, d\tau. \qquad \text{(B.49)}$$

Differentiating with respect to time then gives

$$\mu \frac{d}{dt}\left(\frac{V_\zeta}{\zeta}\right) = -\frac{1}{\zeta^2} \frac{d\zeta}{dt} \int_{\beta(\zeta)}^{t} [P(\tau) - P_0]\, d\tau + \frac{1}{\zeta}[P(t) - P_0]$$

$$+ \frac{d\beta}{d\zeta} \frac{d\zeta}{dt} \left\{ \frac{P_0 - P(\beta(\zeta))}{\zeta} + \frac{[P(\beta(\zeta)) - P_0]^{3/2}}{L\sqrt{3(P_y - P_0)}} \right\}. \qquad \text{(B.50)}$$

From Eq. B.44 we have

$$P(\beta(\zeta)) = P_0 + 3(P_y - P_0) \frac{L^2}{\zeta^2}, \qquad \text{(B.51)}$$

so that Eq. B.50 becomes

$$\mu \frac{d}{dt}\left(\frac{V_\zeta}{\zeta}\right) = -\frac{1}{\zeta^2} \frac{d\zeta}{dt} \int_{\beta(\zeta)}^{t} [P(\tau) - P_0]\, d\tau + \frac{1}{\zeta}[P(t) - P_0]. \qquad \text{(B.52)}$$

Eliminating $\mu(d/dt)(V_\zeta/\zeta)$ between Eqs. B.34c and B.52 results in

$$2\zeta \frac{d\zeta}{dt} \int_{\beta(\zeta)}^{t} [P(\tau) - P_0]\, d\tau + \zeta^2(P - P_0) - 3L^2(P_y - P_0) = 0. \qquad \text{(B.53)}$$

The solution to Eq. B.53 satisfying the initial condition that $\beta(\zeta_{max}) = t_{max}$ is

$$\zeta^2 \int_{\beta(\zeta)}^{t} [P(\tau) - P_0]\, d\tau = 3L^2(P_y - P_0)[t - \beta(\zeta)],$$

$$t_{max} \le t \le t_c. \qquad \text{(B.54)}$$

Equation B.54 gives the hinge-circle motion for the time interval $t_{max} \le t \le t_c$. The motion ceases at $t_c$ when $\zeta(t_c) = L$; since $\beta(L) = t_b$, $t_c$ is found from

$$\int_{t_b}^{t_c} P(\tau)\, d\tau = P_b(t_c - t_b). \tag{B.55}$$

As in the plate solution, the average pressure over the interval of the hinge-band motion is the pressure at which the band is initiated.

The velocity distribution outside the hinge band will be found next. Using Eqs. B.31 and B.49, we have

$$\mu V(z,t) = \frac{z}{\zeta} \int_{\beta(\zeta)}^{t} [P(\tau) - P_0]\, d\tau + \frac{z}{L\sqrt{3(P_y - P_0)}} \int_{t_b}^{\beta(\zeta)} [P(\tau) - P_0]^{3/2}\, d\tau + \frac{3z}{2L} \int_{t_y}^{t_b} [P(\tau) - P_y]\, d\tau, \quad 0 \le z \le \zeta, \quad t_{max} \le t \le t_c. \tag{B.56}$$

An alternative expression which is easier to use to determine the displacement can be derived by considering

$$V(z,t) = z \int_{t_{max}}^{t} \frac{d}{d\tau}\left(\frac{V\zeta}{\zeta}\right) d\tau + V(z,t_{max}), \tag{B.57}$$

which is obtained by integrating Eq. B.31. The integrand is given by Eq. B.34c and $V(z,t_{max})$ is found from Eq. B.41. Making these substitutions, we arrive at

$$V(z,t) = \frac{z}{L}\left[\frac{3}{2} \int_{t_{max}}^{t} \left\{[P(\tau) - P_0]\, \frac{L}{\zeta(\tau)} - (P_y - P_0)\, \frac{L^3}{\zeta^3(\tau)}\right\} d\tau + \frac{1}{\sqrt{3(P_y - P_0)}} \int_{t_b}^{t_{max}} [P(\tau) - P_0]^{3/2}\, d\tau + \frac{3}{2} \int_{t_y}^{t_b} [P(\tau) - P_y]\, d\tau\right],$$

$$0 \le z \le \zeta, \quad t_{max} \le t \le t_c. \tag{B.58}$$

The displacement in the region $\zeta_{max} \leq z \leq \zeta(t)$ is found from

$$W(z,t) = \int_{t_{max}}^{t_z} V(z,\tau)\, d\tau + \int_{t_z}^{t} V(z,\tau)\, d\tau + W(z,t_{max}), \qquad (B.59)$$

where $t = t_z$ when $\zeta(t) = z$. By Eq. B.54, $t_z$ is found from

$$z^2 \int_{\beta(z)}^{t_z} [P(\tau) - P_0]\, d\tau = 3L^2(P_y - P_0)[t_z - \beta(z)]. \qquad (B.60)$$

In the first integral of Eq. B.59, $z > \zeta$ so that the velocity is given by Eq. B.46; in the second integral, $z < \zeta$ and V is given by Eq. B.58. Making these substitutions, doing the integrations, evaluating $W(z,t_{max})$ from Eq. B.47, and using Eqs. B.34c and B.49, we arrive at

$$\mu W(z,t) = \frac{3z}{2L} \int_{t_z}^{t} (t-\tau)\left\{[P(\tau) - P_0]\, \frac{L}{\zeta(\tau)} - (P_y - P_0)\, \frac{L^3}{\zeta^3(\tau)}\right\} d\tau$$

$$+ \frac{3z}{2L} \int_{t_y}^{t_b} (t-\tau)[P(\tau) - P_y]\, d\tau$$

$$+ \frac{z}{L\sqrt{3(P_y - P_0)}} \int_{t_b}^{\beta(z)} (t-\tau)[P(\tau) - P_0]^{3/2}\, d\tau$$

$$+ \int_{\beta(z)}^{t_z} (t-\tau)[P(\tau) - P_0]\, d\tau, \qquad \zeta_{max} \leq z \leq \zeta(t), \qquad t_{max} \leq t \leq t_c. \qquad (B.61)$$

The displacement in the region $0 \leq z \leq \zeta_{max}$ can be written

$$W(z,t) = \int_{t_{max}}^{t} V(z,\tau)\, d\tau + W(z,t_{max}). \qquad (B.62)$$

In the integral, $z < \zeta$ so that V is given by Eq. B.58; $W(z,t_{max})$ is evaluated from Eq. B.42. Making these substitutions into Eq. B.62 and performing the integration, we arrive at

$$\mu W(z,t) = \frac{3z}{2L}\int_{t_{max}}^{t}(t-\tau)\left\{[P(\tau)-P_0]\frac{L}{\zeta(\tau)} - (P_y-P_0)\frac{L^3}{\zeta^3(\tau)}\right\}d\tau$$

$$+ \frac{3z}{2L}\int_{t_y}^{t_b}(t-\tau)[P(\tau)-P_y]\,d\tau$$

$$+ \frac{z}{L\sqrt{3(P_y-P_0)}}\int_{t_b}^{t_{max}}(t-\tau)[P(\tau)-P_0]^{3/2}\,d\tau,$$

$$0 \le z \le \zeta_{max}, \qquad t_{max} \le t \le t_c. \tag{B.63}$$

The appropriate discontinuity conditions are satisfied by the solution in the interval $t_{max} \le t \le t_c$. From Eqs. B.34d and B.53, we have that

$$\left.\frac{\partial^2 M_z}{\partial z^2}\right|_{z=\zeta-} = -\frac{1}{\zeta}\frac{d\zeta}{dt}\int_{\beta(\zeta)}^{t}[P(\tau)-P_0]\,d\tau. \tag{B.64}$$

Since $\zeta$ increases in this time interval and the integral is nonnegative, inequality B.35 holds and the yield condition is not violated in the region $0 \le z \le \zeta$.

The velocity and displacement distributions at $t_c$ are, from Eqs. B.56, B.61, B.63, and B.55,

$$\left.\begin{aligned}
&\mu V(z,t_c) = \frac{3z}{2L}\int_{t_y}^{t_c}[P(\tau)-P_y]\,d\tau, \qquad 0 \le z \le L,\\
&\mu W(z,t_c) = \frac{3z}{2L}\int_{t_z}^{t_c}(t_c-\tau)\left\{[P(\tau)-P_0]\frac{L}{\zeta(\tau)} - (P_y-P_0)\frac{L^3}{\zeta^3(\tau)}\right\}d\tau + \frac{3z}{2L}\int_{t_y}^{t_b}(t_c-\tau)[P(\tau)-P_y]\,d\tau\\
&\qquad + \frac{z}{L\sqrt{3(P_y-P_0)}}\int_{t_b}^{\beta(z)}(t_c-\tau)[P(\tau)-P_0]^{3/2}\,d\tau + \int_{\beta(z)}^{t_z}(t_c-\tau)[P(\tau)-P_0]\,d\tau,\\
&\qquad \zeta_{max} \le z \le L,
\end{aligned}\right\} \tag{B.65}$$

and

$$\left.\begin{aligned}
&\mu W(z,t_c) = \frac{3z}{2L}\int_{t_{max}}^{t_c}(t_c-\tau)\left\{[P(\tau)-P_0]\frac{L}{\zeta(\tau)} - (P_y-P_0)\frac{L^3}{\zeta^3(\tau)}\right\}d\tau\\
&\qquad + \frac{3z}{2L}\int_{t_y}^{t_b}(t_c-\tau)[P(\tau)-P_y]\,d\tau + \frac{z}{L\sqrt{3(P_y-P_0)}}\int_{t_b}^{t_{max}}(t_c-\tau)[P(\tau)-P_0]^{3/2}\,d\tau,\\
&\qquad 0 \le z \le \zeta_{max}.
\end{aligned}\right\}$$

In particular, at $z = L$ where $t_z = t_c$ and $\beta(z) = t_b$, we have

$$\mu V_L(t_c) = \frac{3}{2}\int_{t_y}^{t_c} [P(\tau) - P_y]\, d\tau \tag{B.66a}$$

and

$$\mu W_L(t_c) = \frac{3}{2}\int_{t_y}^{t_b} (t_c - \tau)[P(\tau) - P_y]\, d\tau + \int_{t_b}^{t_c} (t_c - \tau)[P(\tau) - P_0]\, d\tau. \tag{B.66b}$$

d. Interval $t_c \le t \le t_f$

Since the hinge band has disappeared, Eqs. B.13, B.15c, and B.15d apply in this interval as they did in the initial interval $t_y \le t \le t_b$. After performing straightforward integrations with respect to time, we have, using Eq. B.66a,

$$\mu V(z,t) = \frac{3z}{2L}\int_{t_y}^{t} [P(\tau) - P_y]\, d\tau \tag{B.67a}$$

and

$$\mu W(z,t) = \frac{3z}{2L}\left\{\int_{t_y}^{t} (t - \tau)[P(\tau) - P_y]\, d\tau - \int_{t_y}^{t_c} (t_c - \tau)[P(\tau) - P_y]\, d\tau\right\} + \mu W(z,t_c), \quad 0 \le z \le L, \quad t_c \le t \le t_f. \tag{B.67b}$$

In particular,

$$\mu V_L(t) = \frac{3}{2}\int_{t_y}^{t} [P(\tau) - P_y]\, d\tau \tag{B.68a}$$

and

$$\mu W_L(t) = \frac{3}{2}\int_{t_y}^{t} (t - \tau)[P(\tau) - P_y]\, d\tau - \frac{3}{2}\int_{t_b}^{t_c} (t_c - \tau)[P(\tau) - P_y]\, d\tau + \int_{t_b}^{t_c} (t_c - \tau)[P(\tau) - P_0]\, d\tau, \quad t_c \le t \le t_f. \tag{B.68b}$$

The time $t_f$ when the deformation ceases is determined from Eq. B.67a to be given by

$$\int_{t_y}^{t_f} P(\tau)\, d\tau = P_y(t_f - t_y), \tag{B.69}$$

which is identical to Eq. B.25. As in the plate solution, the average pressure during the deformation is the yield pressure.

Evaluating $W_L(t_f)$ from Eq. B.68b, using Eqs. B.23, B.55 and B.69, we have, after some algebraic rearrangement,

$$\mu W_L(t_f) = \frac{3}{4P_y}\left[\int_{t_y}^{t_f} P(\tau)\, d\tau\right]^2 - \frac{3}{2}\int_{t_y}^{t_f} (\tau - t_y)\, P(\tau)\, d\tau$$

$$- \frac{1}{4P_b}\left[\int_{t_b}^{t_c} P(\tau)\, d\tau\right]^2 + \frac{1}{2}\int_{t_b}^{t_c} (\tau - t_b)\, P(\tau)\, d\tau. \tag{B.70}$$

Using definitions A.22 and A.78 for I, $P_e$, I*, and $P_e^*$, the expression for the final displacement can be written

$$W_L(t_f) = \frac{I^2}{4\mu P_y}\left[3\left(1 - \frac{P_y}{P_e}\right) - \left(\frac{I^*}{I}\right)^2\left(\frac{P_y}{P_b} - \frac{P_y}{P_e^*}\right)\right]. \tag{B.71}$$

# APPENDIX C

## Beam Subject to Transverse Dynamic Load of General Pulse Shape

### 1. Introduction

The dynamic plastic deformation of an unsupported beam subjected to a concentrated transverse force at its center is treated by Symonds.[1] He exhibits numerical results for the rectangular, triangular, and half-sine pulse shapes shown in Fig. 1b, 1e, and 1f. Additional results for these shapes and for the linear and exponential decay shapes of Fig. 1c and 1d were obtained for this report. The derivation of the governing differential equations is divided between Refs. 1 and 11. Accordingly, the important features of the derivation will be summarized here.

### 2. Statement of Problem

Consider the free-free beam shown in Fig. 2c having length 2L and mass $\gamma$ per unit length. The beam material is assumed to rigid, perfectly plastic with yield moment $M_0$.

Under the action of a concentrated force $F(t)$ at its center, the beam may proceed through several different types of motion depending on the pulse magnitude and shape. These types of motion and the corresponding governing equations are discussed below.

Let $v(x,t)$ and $w(x,t)$ be the total velocity and displacement of the beam and $V(x,t)$ and $W(x,t)$ be the velocity and displacement produced by plastic deformation, all measured positive in the direction of the force. Then,

$$\left.\begin{aligned} V(x,t) &= v(0,t) - v(L,t) \\ \text{and} \\ W(x,t) &= w(0,t) - w(L,t) \end{aligned}\right\}. \qquad (C.1)$$

Consequently, $w(L,t)$ is the rigid body motion of the beam, while $W(x,t)$ is its plastic deformation measured from a line through the ends of the beam, with $W(0,t)$ being the maximum deformation. We will write

$$\left.\begin{aligned} v_0(t) &= v(0,t), \quad v_L(t) = v(L,t), \\ w_0(t) &= w(0,t), \quad w_L(t) = w(L,t), \\ \text{and} \\ V_0(t) &= V(0,t), \quad W_0(t) = W(0,t). \end{aligned}\right\} \qquad (C.2)$$

a. Phase 1. Rigid Body Motion

Until and unless the maximum bending moment in the beam reaches the value $M_0$ at time $t_y$, the beam moves as a rigid body such that

$$\left.\begin{aligned} &v(x,t) = v_0(t), \quad V(x,t) = 0 \\ \text{and} \\ &w(x,t) = w_0(t), \quad W(x,t) = 0, \quad 0 \le t \le t_y \end{aligned}\right\}. \tag{C.3}$$

From Newton's equation of motion, we have

$$F(t) = 2\gamma L \frac{dv_0}{dt}, \tag{C.4}$$

so that integrating gives

$$\left.\begin{aligned} &v_0(t) = \frac{1}{2\gamma L}\int_0^t F(\tau)\, d\tau \\ \text{and} \\ &w_0(t) = \frac{1}{2\gamma L}\int_0^t (t-\tau)\, F(\tau)\, d\tau, \quad 0 \le t \le t_y \end{aligned}\right\}. \tag{C.5}$$

The bending moment in the right half of the beam is given by, using D'Alembert's principle,

$$M(x,t) = -\frac{1}{2}\gamma(L-x)^2 \frac{dv_0}{dt}, \tag{C.6}$$

or, using Eq. C.4,

$$M(x,t) = -\frac{(L-x)^2}{4L} F(t), \quad 0 \le t \le t_y. \tag{C.7}$$

The maximum magnitude of the bending moment is at the center of the beam. Since the time $t_y$ is when yielding first occurs,

$$M(0,t_y) = -M_0, \tag{C.8}$$

so that, from Eqs. C.7 and C.8,

$$F_y = \frac{4M_0}{L}. \tag{C.9}$$

b. Phase 2. Rigid Body Motion Plus Rotation about Center Plastic Hinge

At $t_y$ a plastic hinge forms at $z = 0$ and a rotation of the two rigid halves of the beam about its center is added to the rigid body motion. Only the right half of the beam will be considered here.

The equations of translation and rotation of the right half of the beam are

$$\left.\begin{aligned} \tfrac{1}{2}F &= L\frac{dv_c}{dt} \\ \text{and} \\ \tfrac{1}{4}FL - M_0 &= \frac{1}{12}\gamma L^3 \frac{d\omega}{dt} \end{aligned}\right\}, \qquad (C.10)$$

where $\omega$ is the angular velocity of the right half, measured positive clockwise, and $v_c$ is the velocity of the center of mass of the right half. Integration of Eqs. C.10 gives, using Eqs. C.5 and C.9,

$$\left.\begin{aligned} v_c &= \frac{1}{2\gamma L}\int_0^t F(\tau)\, d\tau, \\ \omega &= \frac{3}{\gamma L^2}\int_{t_y}^t [F(\tau) - F_y]\, d\tau. \end{aligned}\right\} \qquad (C.11)$$

Since

$$v_0 = v_c + \tfrac{1}{2}\omega L$$

and

$$v_L = v_c - \tfrac{1}{2}\omega L, \qquad (C.12)$$

we have

$$\left.\begin{aligned} V_0(t) &= \omega L \\ &= \frac{3}{\gamma L}\int_{t_y}^t [F(\tau) - F_y]\, d\tau \\ \text{and} \\ W_0(t) &= \frac{3}{\gamma L}\int_{t_y}^t (t - \tau)[F(\tau) - F_y]\, d\tau \end{aligned}\right\}. \qquad (C.13)$$

If no other plastic hinges form, the plastic deformation of the beam is entirely in Phase 2. The time $t_f$ when the plastic deformation ends is found from

$$V_0(t_f) = 0, \qquad t_f > t_y. \tag{C.14}$$

By Eqs. C.13 and C.14, $t_f$ is determined from

$$\int_{t_y}^{t_f} F(\tau)\, d\tau = F_y(t_f - t_y), \tag{C.15}$$

so that, as in the circular-plate and reinforced-circular-shell problems, the average value of the load during deformation is the yield load. Define impulse I per unit length, mean time $t_{mean}$, and effective force $F_e$ of the pulse through

$$\left.\begin{aligned} I &= \int_{t_y}^{t_f} F(\tau)\, d\tau, \\ t_{mean} &= \frac{1}{I}\int_{t_y}^{t_f} (\tau - t_y)\, F(\tau)\, d\tau, \end{aligned}\right\} \tag{C.16}$$

and

$$F_e = \frac{I}{2t_{mean}}.$$

Then from Eqs. C.13, C.15, and C.16, we have for the final maximum plastic deformation of the beam

$$W_0(t_f) = \frac{3I^2}{2\gamma L F_y}\left(1 - \frac{F_y}{F_e}\right). \tag{C.17}$$

The bending moment in the right half of the beam is found by again using D'Alembert's principle to load the beam with inertia forces. The result is

$$M(x,t) = -\frac{1}{2}\gamma(L-x)^2\frac{dv_c}{dt} + \frac{1}{12}\gamma(L-x)^2(L+2x)\frac{d\omega}{dt}, \tag{C.18}$$

or, using Eqs. C.10,

$$M(x,t) = \frac{(L-x)^2}{4L^2}\left[2xF(t) - (L+2x)\,F_y\right]. \tag{C.19}$$

The moment is a minimum at $x = 0$ and is zero at $x = L$ and $x = \frac{1}{2}LF_y/(F - F_y)$; consequently, it has a maximum at some point $x_m$ between the zeros. If $M(x_m,t)$ reaches the value $M_0$ at some time $t_h$, then another plastic hinge will form at $x_m$. Differentiating Eq. C.19 gives

$$\frac{\partial M}{\partial x} = \frac{L - x}{2L^2}[(L - 3x)\,F(t) + 3xF_y], \tag{C.20}$$

so that

$$x_m = \frac{FL}{3(F - F_y)}. \tag{C.21}$$

Therefore,

$$M(x_m,t) = \frac{L(2F - 3F_y)^3}{108(F - F_y)^2}. \tag{C.22}$$

Let

$$M(\xi_h,t_h) = M_0, \tag{C.23}$$

so that a hinge forms at $x = \xi_h$ at time $t_h$. Then $F_h[=F(t_h)]$ is the solution of, using Eqs. C.22, C.23, and C.9,

$$8F_h^3 - 63F_yF_h^2 + 108F_y^2F_h - 54F_y^3 = 0, \tag{C.24}$$

while

$$\xi_h = \frac{F_hL}{3(F_h - F_y)}. \tag{C.25}$$

The numerical solution of cubic equation C.24 yields

$$F_h = 5.7218F_y,$$

$$\xi_h = 0.4039L. \tag{C.26}$$

If $F_{max} > F_h$, outer hinges form initially at $x = \pm\xi_h$.

c. Phase 3. Rigid Body Motion Plus Rotation about Center and Outer Plastic Hinges

In Phase 3, the beam is composed of four rigid sections which rotate about plastic hinges at the origin and $\pm\xi(t)$ and which also translate as a unit with velocity $v_L(t)$.

Again considering the right half of the beam only, take $\omega_0$ and $v_{c0}$ as the angular velocity and velocity of the center of mass, respectively, of the beam section $0 \leq x \leq \xi$, and take $\omega_1$ and $v_{c1}$ as the corresponding quantities for the section $\xi \leq x \leq L$. The equations of motion are then

$$\left.\begin{aligned} \tfrac{1}{2}F &= \gamma\xi \frac{dv_{c0}}{dt}, \\ \tfrac{1}{4}F\xi - 2M_0 &= \frac{1}{12}\gamma\xi^3 \frac{d\omega_0}{dt}, \\ 0 &= \gamma(L-\xi)\frac{dv_{c1}}{dt}, \end{aligned}\right\} \qquad (C.27)$$

and

$$M_0 = \frac{1}{12}\gamma(L-\xi)^3 \frac{d\omega_1}{dt}.$$

Since

$$\left.\begin{aligned} \frac{dv_0}{dt} &= \frac{dv_{c0}}{dt} + \frac{1}{2}\xi\frac{d\omega_0}{dt} \\ \text{and} \\ \frac{dv_L}{dt} &= \frac{dv_{c1}}{dt} - \frac{1}{2}(L-\xi)\frac{d\omega_1}{dt} \end{aligned}\right\}, \qquad (C.28)$$

the differential equations that determine the shape of the plastically deformed beam are

$$\left.\begin{aligned} \gamma\frac{dV_0}{dt} &= \frac{2F}{\xi} - \frac{3LF_y}{\xi^2} + \frac{3LF_y}{2(L-\xi)^2}, \\ \gamma\frac{d\omega_0}{dt} &= \frac{3F}{\xi^2} - \frac{6LF_y}{\xi^3}, \\ \gamma\frac{d\omega_1}{dt} &= \frac{3LF_y}{(L-\xi)^3}, \\ \text{and} \\ \frac{dW_0}{dt} &= V_0. \end{aligned}\right\} \qquad (C.29)$$

However, the hinge position $\xi(t)$ is still an unknown quantity and must be determined before Eqs. C.29 can be solved.

The discontinuity in the acceleration $\partial v/\partial t$ across a moving plastic hinge at $\xi(t)$ is shown in Ref. 11 to be given by

$$\left.\frac{\partial v}{\partial t}\right|_{\xi+} - \left.\frac{\partial v}{\partial t}\right|_{\xi-} + \frac{d\xi}{dt}\left[\left.\frac{\partial v}{\partial \xi}\right|_{\xi+} - \left.\frac{\partial v}{\partial \xi}\right|_{\xi-}\right] = 0. \tag{C.30}$$

Since

$$\left. v \right|_{\xi-} = v_{c0} - \tfrac{1}{2}\xi\omega_0$$

and

$$\left. v \right|_{\xi+} = v_{c1} + \tfrac{1}{2}\xi\omega_1, \tag{C.31}$$

we find from Eqs. C.30, C.27, and C.29 that the differential equation for $\xi(t)$ is

$$\frac{d\xi}{dt} = \frac{1}{\gamma(\omega_0 - \omega_1)}\left[\frac{3F_yL}{\xi^2} - \frac{3F_yL}{2(L-\xi)^2} - \frac{F}{\xi}\right]. \tag{C.32}$$

The set of coupled nonlinear differential equations C.29 and C.32 is easily solved on a computer to determine the plastic-deformation history.

Equation C.32 can be integrated in closed form; the result is

$$\gamma\xi^2(3L - 2\xi)(\omega_0 - \omega_1) + \gamma L^3\omega_1 = 3L\int_{t_y}^{t}[F(\tau) - F_y]\,d\tau, \tag{C.33}$$

which can be verified by differentiation, using Eqs. C.29. Equation C.33 can be derived directly from momentum considerations.[1]

The angular velocities $\omega_0$ and $\omega_1$ are equal at $t_h$ when the outer plastic hinge first appears and again at $t_c$ when $\xi$ disappears. From Eq. C.33, we have that

$$\omega(t_c) = \frac{3}{\gamma L^2}\int_{t_y}^{t_c}[F(\tau) - F_y]\,d\tau. \tag{C.34}$$

After $t_c$, differential equations C.10 are applicable again. Consequently,

$$\left.\begin{aligned} \omega(t) &= \frac{3}{\gamma L^2}\int_{t_c}^{t}[F(\tau)-F_y]\,d\tau + \omega(t_c) \\ &= \frac{3}{\gamma L^2}\int_{t_y}^{t}[F(\tau)-F_y]\,d\tau, \qquad t_c \le t \le t_f \end{aligned}\right\}. \tag{C.35}$$

The plastic deformation stops at $t_f$ when $\omega = 0$; $t_f$ is thus found from

$$\int_{t_y}^{t_f} F(\tau)\,d\tau = F_y(t_f - t_y), \tag{C.36}$$

which is identical to Eq. C.15. Therefore, even though differential equations C.29 cannot be solved in closed form, the deformation interval can still be determined, and the form of the equation is unaffected by the occurrence of outer hinges.

The bending moment in the inner portion of the beam in Phase 3 is given by

$$M(x,t) = M_0 - \frac{1}{2}(\xi - x)^2\frac{dv_{c0}}{dt} + \frac{1}{12}\gamma(\xi - x)^2(\xi + 2x)\frac{d\omega_0}{dt}; \tag{C.37}$$

in the outer portion,

$$M(x,t) = -\frac{1}{2}\gamma(L - x)^2\frac{dv_1}{dt} + \frac{1}{12}\gamma(L - x)^2(L + 2x - 3\xi)\frac{d\omega_1}{dt}. \tag{C.38}$$

Using Eqs. C.27 and C.9, we have

$$M(x,t) = \frac{x(\xi - x)^2 F}{2\xi^2} - \frac{L(\xi^3 - 6\xi x^2 + 4x^3)F_y}{4\xi^3}, \qquad 0 \le x \le \xi, \tag{C.39a}$$

and

$$M(x,t) = \frac{L(L - x)^2(L + 2x - 3\xi)F_y}{4(L - \xi)^3}, \qquad \xi \le x \le L. \tag{C.39b}$$

It is easily verified that

$$\left.\begin{aligned} &M(0,t) = -M_0,\ M(\xi,t) = M_0,\ M(L,t) = 0, \\ &\frac{\partial M}{\partial x} = 0 \text{ at } x = \xi, L. \end{aligned}\right\} \tag{C.40}$$

d. Phase 4. Outer Hinge Becomes a Hinge Band

If, during the Phase 3 deformation,

$$\frac{\partial^2 M}{\partial x^2} = 0 \text{ at } x = \xi-, \tag{C.41}$$

a hinge band would begin to form at $\xi$. This is because at slightly higher loads Eq. C.39a would predict a saddle point at $\xi$ with M exceeding $M_0$ to the left of $\xi$. By Eq. C.39a, we have that Eq. C.41 is equivalent to

$$F(t)\xi(t) = 3F_y L. \tag{C.42}$$

Phase 4 motion does not occur for the load ranges presented in the results of this report (see discussion in Ref. 1).

REFERENCES


1. P. S. Symonds, *Dynamic Load Characteristics in Plastic Bending of Beams*, J. Appl. Mech. *20*(4), 475-481 (1953).

2. P. G. Hodge, Jr., *The Influence of Blast Characteristics on the Final Deformation of Circular Cylindrical Shells*, J. Appl. Mech. *23*(4), 617-624 (1956).

3. P. P. Perzyna, *Dynamic Load Carrying Capacity of a Circular Plate*, Arch. Mech. Stosow. *10*(5), 635-647 (1958).

4. H. G. Hopkins and W. Prager, *On the Dynamics of Plastic Circular Plates*, J. Appl. Math. Phys. *5*(4), 317-330 (1954).

5. G. Eason and R. T. Shield, *Dynamic Loading of Rigid-Plastic Cylindrical Shells*, J. Mech. Phys. Solids *4*(2), 53-71 (1956).

6. C. K. Youngdahl, "The Equivalence of Dynamic Loads for the Final Plastic Deformation of a Tube," *Proc. First Int. Conf. on Pressure Vessel Technology*, CONF-690906 (Oct 1969), Vol. 1, pp. 89-100.

7. C. K. Youngdahl, *The Dynamic Plastic Response of a Tube to an Impulsive Ring Load of Arbitrary Pulse Shape*, ANL-7562 (Apr 1969).

8. H. G. Hopkins and W. Prager, *The Load Carrying Capacity of Circular Plates*, J. Mech. Phys. Solids *2*(1), 1-13 (1953).

9. M. F. Conroy, *Rigid-Plastic Analysis of a Simply Supported Circular Plate Due to Dynamic Circular Loading*, J. Franklin Inst. *288*(2), 121-135 (1969).

10. Y. V. Nemirovsky and V. N. Mazalov, *Dynamic Behavior of Cylindrical Shells Strengthened with Ring Ribs--Part I: Infinitely Long Shell*, Int. J. Solids Struct *5*(8), 817-832 (1969).

11. E. H. Lee and P. S. Symonds, *Large Plastic Deformations of Beams Under Transverse Impact*, J. Appl. Mech. *19*(3), 308-313 (1952).